

## FORUM REVIEW ARTICLE

---

# Challenges and Opportunities for Small-Molecule Fluorescent Probes in Redox Biology Applications

Xiqian Jiang,<sup>1</sup> Lingfei Wang,<sup>1</sup> Shaina L. Carroll,<sup>1</sup> Jianwei Chen,<sup>1</sup> Meng C. Wang,<sup>2,3</sup> and Jin Wang<sup>1,4,5</sup>

### Abstract

**Significance:** The concentrations of reactive oxygen/nitrogen species (ROS/RNS) are critical to various biochemical processes. Small-molecule fluorescent probes have been widely used to detect and/or quantify ROS/RNS in many redox biology studies and serve as an important complementary to protein-based sensors with unique applications.

**Recent Advances:** New sensing reactions have emerged in probe development, allowing more selective and quantitative detection of ROS/RNS, especially in live cells. Improvements have been made in sensing reactions, fluorophores, and bioavailability of probe molecules.

**Critical Issues:** In this review, we will not only summarize redox-related small-molecule fluorescent probes but also lay out the challenges of designing probes to help redox biologists independently evaluate the quality of reported small-molecule fluorescent probes, especially in the chemistry literature. We specifically highlight the advantages of reversibility in sensing reactions and its applications in ratiometric probe design for quantitative measurements in living cells. In addition, we compare the advantages and disadvantages of small-molecule probes and protein-based probes.

**Future Directions:** The low physiological relevant concentrations of most ROS/RNS call for new sensing reactions with better selectivity, kinetics, and reversibility; fluorophores with high quantum yield, wide wavelength coverage, and Stokes shifts; and structural design with good aqueous solubility, membrane permeability, low protein interference, and organelle specificity. *Antioxid. Redox Signal.* 00, 000–000.

**Keywords:** fluorescent probes, sensing and imaging, hydrogen peroxide, glutathione, reversible reactions, ratiometric

### Introduction

REACTIVE OXYGEN SPECIES (ROS) and reactive nitrogen species (RNS) are generated through intracellular metabolism of oxygen. Oxidative damage to biomolecules, such as DNA, protein, and lipids, as a result of ROS/RNS has been linked to many pathological events (35, 48, 49, 61, 134). In the past decade, there has been increasing evidence that ROS/RNS also serve as important signaling molecules (33, 112, 130). In cells, ROS/RNS establish redox homeostasis with antioxidants, such as glutathione (GSH), cysteine (Cys), NADH, and NADPH, to regulate various biological processes, including development and immune responses (32, 38, 130, 174). ROS/

RNS can be categorized into anions ( $O_2^{\cdot-}$ ,  $ONOO^-$ ,  $OCI^-$ ), radicals ( $\cdot OH$ ,  $ROO\cdot$ ), and neutral molecules ( $H_2O_2$ ,  $^1O_2$ ). Among all the ROS/RNS, the biological functions of hydrogen peroxide are the most extensively studied (136).

In general, there are two classes of methods used for detecting hydrogen peroxide ( $H_2O_2$ ) or other redox signaling molecules in living cells: genetically encoded protein probes and small-molecule-based probes. Genetically encoded protein probes utilize naturally occurring redox-responsive domains for sensing. Several recent review articles, including the ones in this issue, have comprehensively summarized genetically encoded probes for  $H_2O_2$ , GSH, and thioredoxin (6, 9, 12, 44, 46, 47, 105, 108, 114, 125).

---

Departments of <sup>1</sup>Pharmacology and Chemical Biology, <sup>2</sup>Molecular and Human Genetics, <sup>4</sup>Department of Molecular and Cellular Biology, <sup>3</sup>Huffington Center on Aging, and <sup>5</sup>Center for Drug Discovery, Baylor College of Medicine, Houston, Texas.

The best known examples of reaction-based small-molecule probes are the calcium probes developed by Roger Tsien, such as Fura-2 and Indo-1 (150). Since the development of these probes, numerous fluorescence-based small-molecule probes with reaction centers have been developed, especially in the field of redox signaling (14, 22, 53, 68, 145, 159, 166). Due to the high reactivity of most of the redox signaling molecules, the selectivity of the corresponding small-molecule probes still has sufficient room for improvement. Therefore, it remains a challenge to chemically distinguish between similar redox-active small molecules using small-molecule-based probes (164).

As biological research has advanced, an increasing number of redox signaling molecules have been uncovered (130, 136). Popular probes that were once considered selective for their targeted analytes are now known to cross-react with newly discovered redox signaling molecules. For example, dichlorodihydrofluorescein (DCFH) and boronate-based probes were initially considered to be  $H_2O_2$  specific probes. However, recent studies revealed that they cross-react with other species in the redox signaling chain, such as peroxynitrite (70, 137). This will be further discussed in later sections. Therefore, it is very important for redox biologists to fully understand the sensing mechanism and limitations of the probe to draw appropriate conclusions.

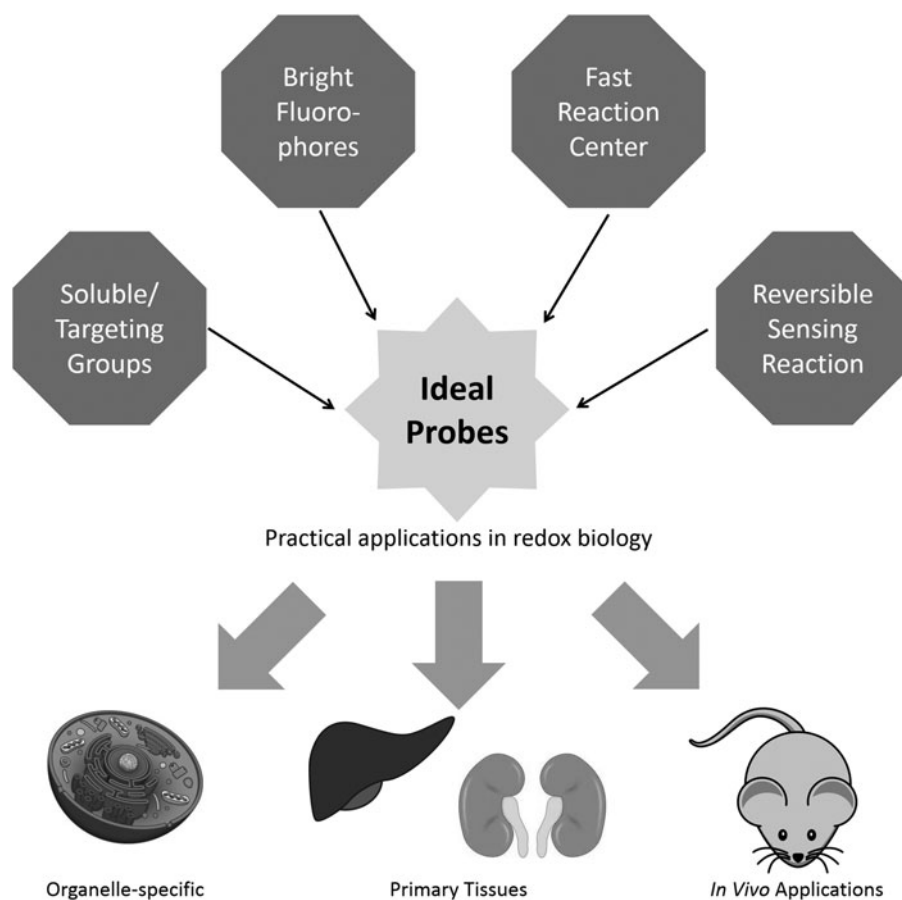
In this review, we will not only summarize redox-related small-molecule fluorescent probes but also lay out the challenges for probe design to help redox biologists independently evaluate the quality of reported small-molecule fluorescent probes.

## Key Challenges for Designing Small-Molecule Fluorescent Probes

### Discovering sensing reactions

Discovering a reaction specific to the intended analyte is fundamental to designing a reaction-based small-molecule probe. In the case of protein-based probes, such as redox-sensitive green fluorescent protein (roGFP) or hydrogen peroxide sensor protein (Hyper), scientists can take advantage of existing sensing moieties from naturally occurring protein structures (105). In contrast, the sensing reactions for small-molecule-based probes mostly originate from “intelligent design.”

Taking hydrogen peroxide as an example, only a few chemical reactions have been reported to detect hydrogen peroxide in living cells. Among the reported  $H_2O_2$  probes, the majority of them are based on the oxidation of boronate esters (111, 145). Other sensing reactions for hydrogen peroxide include oxidation-induced C-C bond cleavage of benzils (2), C-S bond cleavage of perfluoro-benzyl sulfonates (106), and C-N bond cleavage of anilines (82); direct oxidation of phosphorous (138), tellurium (78), and selenium (90, 179); and direct metal chelation by hydrogen peroxide (42). Most of the reaction-based probes have been extensively reviewed (14, 55, 145). Here, we discuss several aspects of the design criteria for ideal probes, including selectivity, kinetics, and reversibility of the sensing reactions (Fig. 1).



**FIG. 1.** Desired features for small-molecule-based fluorescent probes.

### Selectivity of sensing reactions

A selective sensing reaction is the key to designing small-molecule fluorescent probes. It should be noted that we prefer the term “selective” over “specific.” Although specific probes, which react with nothing but the analyte of interest, are always desired, hardly any probes are truly specific due to the complexity of biological systems. Therefore, we prefer to use the term “selective” to describe probes that preferentially react with the desired analyte at physiological conditions. It is important to fully evaluate the reactivity of the designed probe and any analytes that could potentially interfere under physiologically relevant conditions.

Taking the development of  $\text{H}_2\text{O}_2$  probes as an example, DCFH was widely used as an  $\text{H}_2\text{O}_2$  probe (23). However, the complete mechanism for the oxidation of DCFH to dichlorofluorescein (DCF) involves multiple steps and many oxidants are involved, including oxidized glutathione (GSSG), NAD, oxygen ( $\text{O}_2$ ), iron, and nitric oxide ( $\text{NO}\cdot$ ) (70, 71). Therefore, the fluorescent signal changes of DCFH to DCF cannot be solely attributed to changes in  $\text{H}_2\text{O}_2$  levels and, indeed, reflect the overall redox state of the cells.

Advancing from DCFH, several oxidation-induced C-X (X=C, S, or N) bond cleavage reaction-based  $\text{H}_2\text{O}_2$  probes were developed. The first reactive center used for  $\text{H}_2\text{O}_2$  sensing was perfluoro-benzyl sulfonate (106, 172). Fluorophores are linked with quenchers through this cleavable ester bond, enabling fluorogenic responses in the presence of  $\text{H}_2\text{O}_2$ . Unfortunately, the reactivity of these acyl sulfonates toward other ROS was not extensively evaluated, partially due to the lack of knowledge of other redox signaling molecules at the time of probe development. Perfluoro-benzyl sulfonate is prone to reductive and nucleophilic reagents from an organic chemistry perspective. Therefore, strong reductive redox signaling molecules such as hydrogen sulfide ( $\text{H}_2\text{S}$ ) or strong nucleophilic molecules such as cysteine or glutathione are highly likely to react with this reactive moiety.

Recently, Chang and co-workers pioneered the use of boronate esters as selective reductants for  $\text{H}_2\text{O}_2$ , which led to a series of new  $\text{H}_2\text{O}_2$  probes (4, 14, 28, 31, 34, 37, 111). The selectivity of this reaction has been examined against a series of oxidants in cells, including superoxide ( $\text{O}_2\cdot^-$ ),  $\text{NO}\cdot$ , hydroxyl radical ( $\text{OH}\cdot$ ), hypochlorite ( $\text{OCl}^-$ ), ozone ( $\text{O}_3$ ), and singlet oxygen ( $^1\text{O}_2$ ). It should be noted that peroxynitrite ( $\text{ONOO}^-$ ), which is generated intracellularly by nitric oxide and hydroxyl radical, was later shown to react with boronates at a much faster rate (over a million times) than  $\text{H}_2\text{O}_2$  in a pH 7.4 buffer (137). Although the intracellular concentration of peroxynitrite is much lower than that of  $\text{H}_2\text{O}_2$ , care should be taken when interpreting results from boronate probes.

The development of GSH probes faces a similar challenge. There are many free thiol-containing species in the intracellular milieu, including small-molecule thiols and protein thiols. Glutathione, which is usually in the millimolar concentration range, accounts for the majority of small-molecule thiols in eukaryotic cells. However, the concentration of free thiols in proteins can also be as high as the millimolar range, potentially interfering with the readout of GSH probes. To provide a definitive assessment of the selectivity of GSH probes, particularly the intracellular selectivity, our group developed a gel permeation chromatography (GPC)-based assay, which we used in the study of our RealThiol probe (66).

In our protocol, live cells were treated with RealThiol first, then lysed in trichloroacetic acid to prevent the dissociation of RealThiol from protein thiols or small-molecule thiols under diluting conditions. GPC with fluorescence detection was then used to separate probes that had reacted with proteins from those that had reacted with small-molecule thiols. We found that the majority (>90%) of RealThiol had, indeed, reacted with GSH. However, this method cannot be easily applied to  $\text{H}_2\text{O}_2$  probe development as the final products of the reacted probes are the same regardless of the nature of the oxidants. A possible experiment to test  $\text{H}_2\text{O}_2$  probe selectivity is to mix a panel of physiologically relevant oxidants to determine the reaction selectivity. If possible, cell lysate should also be added to the mixture to evaluate any potential interference from intracellular proteins.

### Kinetics of sensing reactions

Ideal sensing reactions should have relatively fast kinetics because the analytes are usually only present in the  $\mu\text{M}$  or even  $\text{nM}$  concentration range. The physiologically relevant concentration of  $\text{H}_2\text{O}_2$ , for example, is 1–100  $\text{nM}$  (136). Considering a typical probe staining concentration of 10  $\mu\text{M}$ , the reaction should have a second-order rate constant of at least  $278 \text{ M}^{-1}\cdot\text{s}^{-1}$  (assuming a constant 100  $\text{nM}$  concentration of  $\text{H}_2\text{O}_2$ ) to ensure sensing results will be available within 1 h, and given the detection limit of the instrument toward the corresponding fluorophore is 1  $\mu\text{M}$ . Longer incubation times usually result in more artifacts, such as re-synthesis of the signaling molecule being detected, metabolic inactivation of probes, probe clearance from cells, and photobleaching of the fluorophores (164).

An ideal sensing reaction should occur in real time or at least be able to achieve a reasonable signal readout within 5 min. Unfortunately, it is often a tradeoff between reaction selectivity and kinetics. Faster reactions are usually correlated with lower energy barriers for oxidation, meaning it may be difficult to maintain reaction selectivity, especially in cases where the sensing reaction is irreversible and there are several molecules in the environment with similar reactivity. Such sensing reactions have not been well established in the development of small-molecule-based  $\text{H}_2\text{O}_2$  probes. Most of the  $\text{H}_2\text{O}_2$  probes reported based on boronates have second-order rate constants of 0.1–1.0  $\text{M}^{-1}\cdot\text{s}^{-1}$ , indicating a typical incubation time of >30 min for detecting a change in  $\text{H}_2\text{O}_2$  concentration of 100  $\mu\text{M}$ , far higher than its physiological concentration (110).

The ultimate goal for redox molecule sensing is to find or design a fast but specific chemical reaction against the analyte of interest (10). Another possibility is to design reversible sensing reactions with proper equilibrium constants to ensure sensors only respond to analytes at their physiologically relevant concentrations. A good example of the implementation of this strategy is the development of glutathione probes. Because glutathione is among the very few nonprotein thiol species present at >1  $\text{mM}$  concentration in eukaryotic cells, it is feasible to develop a reversible sensing reaction that quickly and selectively responds to GSH with little interference from other free thiols. Several groups, including our own, have reported fluorescent probes for real-time imaging of GSH in living cells (17, 66, 101, 151).

### Reversibility of sensing reactions

The reversibility of sensing reactions is a relatively complicated issue, especially for  $\text{H}_2\text{O}_2$  and other ROS/RNS. By definition, a reversible chemical reaction, depending on conditions, can proceed in both the forward and reverse direction. A chemical equilibrium is reached when forward and reverse reactions proceed at equal rates (Fig. 2).

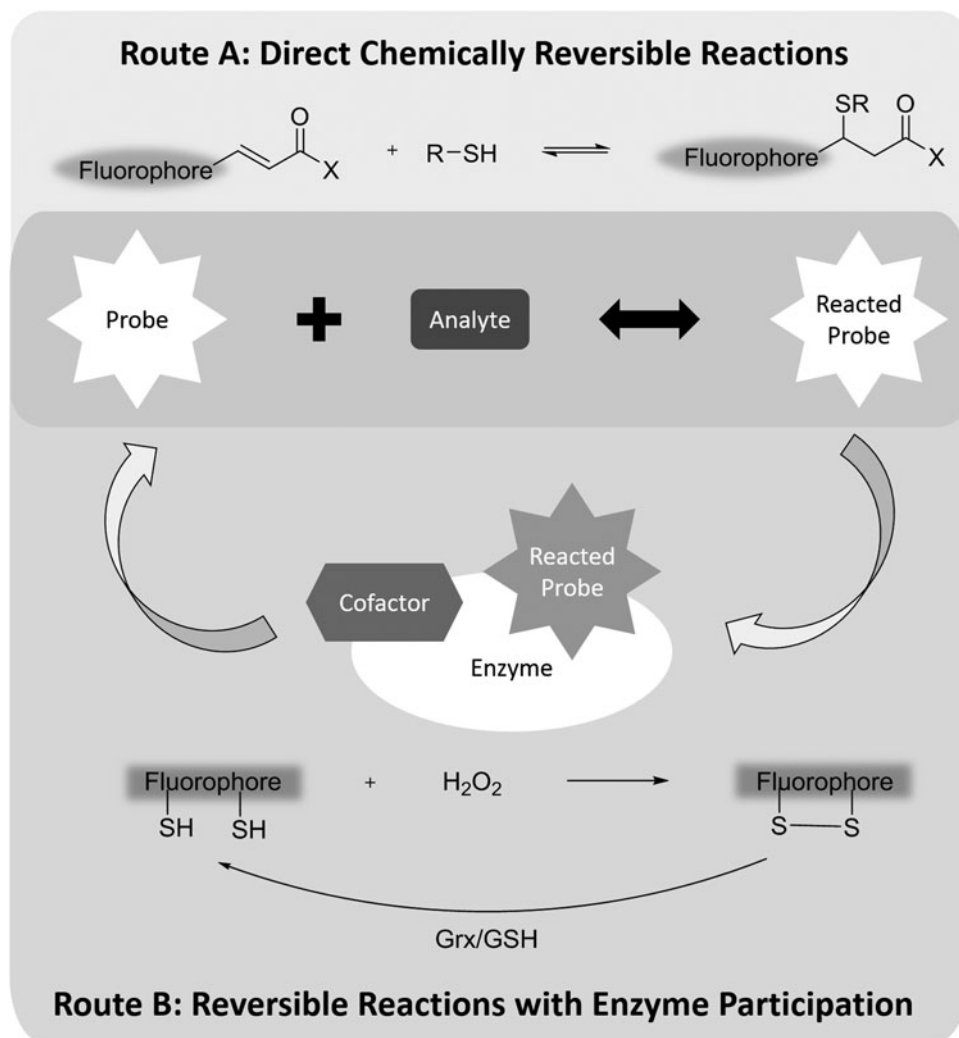
Although irreversible reactions are commonly used in the development of reaction-based fluorescent probes (14), there are a few major advantages to using reversible reactions for probe development. First, because equilibrium is driven by thermodynamics and can be established regardless of the concentration of reactants, it is possible to measure the concentration of an analyte using a probe with a much lower concentration, given there is an appropriate equilibrium constant between the analyte and the probe.

This concept has been well demonstrated in the development of reversible reaction-based GSH probes, in which probes with concentrations in the micromolar or nanomolar range establish equilibria with GSH in the millimolar concentration range (17, 66, 101, 151). If an irreversible reaction-based GSH probe were used, an excess of the probe (above the millimolar concentration of GSH) would have to

be applied to react with all the GSH molecules to obtain a quantitative measurement. Complete scavenging of GSH in cells can trigger oxidative stress, which is undesirable, especially in redox biology studies.

Second, if both reacted and unreacted probes have different fluorescence responses, the concentration of the analyte can be calculated based on the fluorescence ratio of the reacted and unreacted probes at equilibrium conditions. This is usually referred to as “ratiometric” imaging. The key advantage of ratiometric measurement is that its quantification results are independent of the absolute probe concentration in cells. Last but not least, live monitoring or longitudinal tracking of the concentration of an analyte is only feasible by using reversible sensing reactions because irreversible reaction-based probes are saturated over time.

Reversible sensing reactions have been applied to develop probes for several biologically relevant molecules, including calcium and GSH. Because of the complexity of the cellular redox system, oxidation and reduction of these redox probes does not always proceed directly through the same reaction (Fig. 2). For example,  $\text{H}_2\text{O}_2$  protein sensor Hyper transforms to its oxidized form after reacting with  $\text{H}_2\text{O}_2$ . But the oxidized form cannot return to the corresponding reduced form by oxidizing  $\text{H}_2\text{O}$  to  $\text{H}_2\text{O}_2$ . Instead, Hyper utilizes the



**FIG. 2. Two strategies for designing reversible fluorescent probes.** Route A is based on a direct chemical equilibrium between the probe and the analyte, such as in the case of RealThiol glutathione probe. The reversibility of Route B is based on two different chemical reactions. Usually, the reverse reaction is catalyzed by an enzyme, such as in the case of the Hyper hydrogen peroxide probe. Grx, glutaredoxin; GSH, glutathione;  $\text{H}_2\text{O}_2$ , hydrogen peroxide.

glutaredoxin (Grx)/GSH system for its reduction. As long as the reduction capability of the Grx/GSH system is stable, Hyper can be used to determine  $\text{H}_2\text{O}_2$  concentration inside cells at the expense of consuming hydrogen peroxide (105).

Therefore, regarding redox probes, a practical definition of reversible probes should be probes that can monitor both increases and decreases of an analyte in biological systems on the minute-level time scale. Generally, the forward and reverse reactions should proceed at comparable rates under physiological conditions. Increasing the reaction rate between  $\text{H}_2\text{O}_2$  and its protein sensor reduces the limit of detection that the sensor is able to achieve (114). However, it should be noted that blindly pursuing the lowest limit of detection for probe design is not advised. All probes have their own dynamic range of detection. Highly sensitive probes tend to have saturated readouts even at moderate concentrations of the analyte. Therefore, it is important to match the dynamic range of designed probes with the physiological concentration range of the analyte.

Of the small-molecule  $\text{H}_2\text{O}_2$  probes, only a few probes claim applications in monitoring both increases and decreases in  $\text{H}_2\text{O}_2$ , including thiol-disulfide-based and Te/Se, P oxidation-based probes (78, 138, 179, 181). However, the selectivity of these sensing reactions has not been well characterized. As Kaur *et al.* pointed out, these probes would be better described as reflecting “global redox changes” instead of  $\text{H}_2\text{O}_2$  changes (73). To the best of our knowledge, these  $\text{H}_2\text{O}_2$  probes have not been used by redox biologists in their studies.

Several reversible redox probes targeting other ROS/RNS claim to monitor peroxynitrite ( $\text{ONOO}^-$ )/GSH (103),  $\text{O}_2^{\cdot-}$ /GSH (99, 103, 158, 179, 181), and hypochlorous acid ( $\text{HClO}$ )/ $\text{H}_2\text{S}$  (158) “redox couples.” For example, the Han group reported several fluorescent probes for monitoring redox cycles between peroxynitrite and glutathione and defined peroxynitrite and glutathione as a redox couple (103, 179, 181). However, by definition, a redox couple is the two species of a half-reaction involving oxidation or reduction, for example  $\text{Cu}^{2+}/\text{Cu}$ . It is questionable to define  $\text{ONOO}^-$  and GSH as a redox couple.

In Han’s study, the reversibility of the  $\text{ONOO}^-$ /GSH probe was demonstrated by oxidizing the probe with peroxynitrite first, then reducing the probe with addition of GSH. However, peroxynitrite and GSH co-exist in cells. An appropriate test of the reversibility of Han’s probe should be performed in a mixture of peroxynitrite and GSH. In fact, Han’s probe could be potentially used as a reversible peroxynitrite probe. Nonetheless, although the biological meaning of these designed redox couples is elusive, they could be a good starting point for developing new reversible redox probes that oxidize and reduce through different mechanisms.

In summary, reversible sensing reactions have several distinct advantages, although the design of them can be challenging. GSH probes are a unique case; they have been successfully developed to reversibly react with their analyte to achieve quantitative real-time imaging. It may not be trivial to replicate the success of GSH probes to discover similar reversible reactions for highly energetic ROS/RNS. Chemists could potentially mimic protein sensors, such as Hyper, by designing small-molecule probes that can be oxidized by ROS/RNS and reduced by endogenous enzymatic systems. Regardless, new reversible reactions for the sensing

of other ROS/RNS that enable real-time monitoring of redox signals are still in great demand.

#### *Comparison between protein-based probes and small-molecule probes*

Two types of protein-based probes are widely used in redox biology, roGFPs (39, 60) and Hyper (9)-based sensors. roGFPs are often used for measuring GSH redox potentials, and Hyper-based sensors are often used for measuring hydrogen peroxide. Their sensing reactions are based on thiol to disulfide transformations that induce changes in fluorescent protein conformations and, thus, spectral properties. Both reactions are intrinsically reversible and can be used for quantitative measurements.

There are several main advantages to protein-based genetically encoded probes, including high selectivity and sensitivity, amenability to subcellular targeting, and applicability to tissue-specific or whole-body imaging in animals. Despite these advantages, genetically encoded probes are relatively laborious to work with due to the cell transfection process, and it is challenging to apply them in primary tissues, such as patient samples. In addition, high expression of sensor proteins may alter cellular redox state due to rapid consumption of the corresponding analytes. Therefore, it is important to minimize the expression level of sensor proteins to avoid artifacts.

In contrast, small-molecule probes can be a great complement to genetically encoded probes due to their convenience, applicability in primary tissues, and minimal perturbation to the interrogated biological system (if a nanomolar to low micromolar probe concentration is used).

Since  $\text{H}_2\text{O}_2$  probes are available in both protein- and small-molecule-based versions, it provides a fair battleground for comparing these two sensing strategies. Small-molecule  $\text{H}_2\text{O}_2$  probes are mostly used to detect large  $\text{H}_2\text{O}_2$  changes in cells, such as the change that occurs under strong exogenous stimulation with bolus treatment of highly concentrated  $\text{H}_2\text{O}_2$  (15, 106). Although these probes provide information on cellular responses under extreme conditions, they do not have sufficient sensitivity to detect basal levels of  $\text{H}_2\text{O}_2$ .

Protein-based probe Hyper is much better at monitoring subtle concentration changes in  $\text{H}_2\text{O}_2$  (9). In addition, Morgan *et al.* recently reported a highly sensitive peroxiredoxin-based probe that can detect basal levels of  $\text{H}_2\text{O}_2$ , in the low nanomolar to high picomolar range (114). Compared with small-molecule-based  $\text{H}_2\text{O}_2$  probes, their protein-based counterparts have superior sensitivity, dynamic ranges, reaction kinetics, and selectivity. More importantly, protein-based  $\text{H}_2\text{O}_2$  probes are reversible and can provide quantitative measurements of  $\text{H}_2\text{O}_2$  levels in living cells, whereas all small-molecule probes are based on irreversible reactions and can only provide qualitative assessment of large changes of more than  $100 \mu\text{M}$  increase in  $\text{H}_2\text{O}_2$  levels. Therefore, it is not surprising that redox biologists prefer protein-based hydrogen peroxide probes in their studies.

Protein-based and small-molecule-based glutathione probes provide different but complementary measurements. roGFP-based probes such as roGFP1/2 and Grx1-roGFP2 measure GSH redox potentials, which are proportional to the value of  $[\text{GSH}]^2/[\text{GSSG}]$  (39, 60). In contrast, state-of-the-art small-molecule-based GSH probes provide direct measurements of  $[\text{GSH}]$  (66, 101, 151). To the best of our knowledge, there are

no probes available that can quantify GSSG concentrations, either protein or small-molecule based. A possible work-around to measure [GSSG] in living cells is to apply both roGFPs and reversible small-molecule GSH probes simultaneously, then calculate [GSSG] based on the values of  $[GSH]^2/[GSSG]$  and [GSH].

Protein-based redox probes have been further developed by incorporating unnatural amino acids. The Ai group has been a pioneer in this area and recently reported genetically encoded fluorescent probes for peroxynitrite (26) and hydrogen sulfide (19). It should be noted that the protein-based probes reported by the Ai group are based on irreversible reactions with the corresponding analytes, meaning that it would be difficult to obtain quantitative measurements from their readouts or to follow dynamic changes in analyte concentrations.

We have summarized some of the key factors that redox biologists need to consider while choosing between these two types of sensors in Table 1. In our opinion, for basic cell biology studies, protein-based reversible probes, if available, should be preferred due to their superiority in quantitative measurements and real-time monitoring. Small-molecule fluorescent probes become useful when studying primary tissues or when the corresponding protein-based probe is unavailable. Further, we believe that probe developers from both small-molecule and protein camps need to learn from each other and come up with new ideas for redox sensing that can address untapped biological questions.

#### Ideas for designing new reactions

As combinatorial chemistry and high-throughput screening has advanced in recent years, these cutting-edge techniques have been applied in probe design (152, 153). Ahn *et al.* pioneered the use of a target-based combinatorial rosamine library

in searching for GSH probes (3). Schiedel *et al.* introduced a diversity orientated library for screening and discovered a set of bright coumarin-based fluorophores (131). Xie *et al.* designed a screen and discovered several new sensing reactions for biothiols, which brought insights into the future design of sensing reactions (168). In terms of  $H_2O_2$  probe design, we are unaware of similar screening strategies being applied. In general, a well-controlled screen is much more efficient than testing sensing reactions one at a time, especially under physiologically relevant complex conditions.

#### Choosing Appropriate Fluorophores

##### Quantum yields of fluorophores

For any fluorophore, quantum yield is always among the most important characteristics. A high quantum yield can significantly reduce the amount of fluorophore that is necessary to administer to cells. In the case of detecting redox signaling molecules, low probe loading reduces consumption of the analyte of interest, minimizing interference to the biological system being interrogated. Currently, quantum yields of fluorophores have to be determined experimentally, which often requires laborious synthesis.

The Lavis group recently reported a general method to improve quantum yields in several of the most commonly used fluorophores, which greatly advanced the imaging field (52, 54). Their elegant strategy replaced the freely rotating di-alkyl groups, which occur in many fluorophores, with a structurally rigid azetidine group, reducing rotation-related nonradiative energy relaxation process to enhance quantum yields.

Several new strategies, including aggregation induced emission (AIE) and excited state intramolecular proton transfer (ESIPT), provide potentially useful mechanisms for altering quantum yields.

TABLE 1. COMPARISON BETWEEN PROTEIN SENSORS AND SMALL-MOLECULE SENSORS

Name	Analyte	Sensing reaction	Selectivity	Time resolution of sensing	Fluorophores	References
Representative protein sensors						
roGFP1/2	Redox potential $[GSSG]/[GSH]^2$	Thiol-disulfide exchange	Mediated by protein binding	1–10 min	GFP	(39)
Grx1-roGFP2	Redox potential $[GSSG]/[GSH]^2$	Grx thiol-disulfide exchange	Mediated by protein binding	<1 min	GFP	(60)
Hyper	$H_2O_2$	OxyR-RD thiol-disulfide exchange	Mediated by protein binding	5–10 min	cpYFP	(9)
Representative small-molecule sensors						
RealThiol	GSH	Reversible Michael addition	Mediated by appropriate chemical equilibrium	~1 min	High quantum yield coumarin	(66)
QuicGSH	GSH	Reversible nucleophilic addition	Mediated by appropriate chemical equilibrium	<1 min	Rhodamine-Si-Rhodamine FRET pair	(151)
QG-1	GSH	Reversible Michael addition	Mediated by appropriate chemical equilibrium	<1 min	Coumarin	(101)
PF1	$H_2O_2$	Irreversible boronate oxidative cleavage	Mediated by selective chemical reaction	~5 min	Fluorescein	(15)

FRET, Förster resonance energy transfer; Grx, glutaredoxin; GSH, glutathione; GSSG, oxidized glutathione;  $H_2O_2$ , hydrogen peroxide; Hyper, hydrogen peroxide sensor protein; OxyR-RD, regulator domain of *E. Coli* OxyR gene; PF1, peroxyfluor-1; roGFP, redox-sensitive green fluorescent protein.

AIE probe molecules are nonfluorescent at low concentrations, but locally high concentrations of probe molecules induce and self-assemble through  $\pi$ - $\pi$  interactions and trigger luminescence (63). Although sensitive detection of  $\text{H}_2\text{O}_2$  has been demonstrated by using AIE probes in test tube experiments, these probes are difficult to apply in cells (85, 86, 90, 98, 160, 189). To achieve noticeable emission, AIE probes rely on high local concentrations of probe molecules, which can be toxic for cells. Some reported probes even require a loading concentration of up to 1 mM (189). AIE probes are also very hydrophobic due to the indispensable large conjugated building blocks of phenol rings. This can cause solubility and distribution problems in cells, which will be discussed in the following sections.

The ESIPT phenomenon was initially discovered in 3-hydroxyflavone, whose fluorescence relies heavily on intramolecular hydrogen bonding (148, 176). Based on the ESIPT mechanism, several  $\text{H}_2\text{O}_2$  probes were developed and their selectivity was evaluated in test tube experiments (88, 94, 191). However, due to the complex environment inside cells with nearly ubiquitous hydrogen bond donors and acceptors, ESIPT probes may lose most of their excited state energies to the adjacent environment, instead of emitting photons. As Zhao *et al.* pointed out, ESIPT fluorophores prefer aprotic solvents, and “it is still a challenge to use ESIPT molecular probes in protic solvents due to the severe interference of solvents to perturb the ESIPT process” (190).

Current applications of ESIPT redox probes mostly require high percentages of co-solvents or surfactants, resulting in potential artifacts and limited biological significance (94). Further optimization is still required for this type of probe to become practically useful in biological systems.

Quantum dots are another set of emitters developed based on nanoparticle technology. Due to a different emission mechanism than small molecules, quantum dots have extremely high quantum yields and photostability, and their emission is relatively insensitive to environmental changes. Resch-Genger *et al.* extensively reviewed the applications of quantum dots *versus* small-molecule-based probes in cells in detail (126). Several  $\text{H}_2\text{O}_2$  probes based on quantum dots have been reported (56, 89, 129, 133, 185). It should be noted that depending on their sizes and surface charges, quantum dots may enter cells through endocytosis, rendering them uniquely useful for studying  $\text{H}_2\text{O}_2$  signaling in trafficking vesicles.

#### Stokes shift of fluorescent probes

Stokes shift, defined as the difference between excitation maximum and fluorescence emission maximum, is another key factor in determining probe quality. Fluorophores with small Stokes shifts are usually prone to self-quenching, whereas those with large Stokes shifts are usually desired for ratiometric or Förster resonance energy transfer (FRET)-based probes. Coumarin and cyanine fluorophores have intrinsic push-pull structures, leading to potentially large Stokes shifts. However, some of these structures have high molecular weights or high polarity, potentially limiting the cell permeability of the designed probes. A “prodrug” strategy can be applied to enhance cell permeability by converting polar probes into nonpolar pro-probes, which are then processed inside cells to regenerate the parent probes (66).

FRET provides another strategy to design probes with pseudo large Stokes shifts. Several FRET-based  $\text{H}_2\text{O}_2$  probes were reported to have large Stokes shifts (5, 41, 163).

#### Design of ratiometric fluorescent probes

Calcium probe Fura-2, developed by Roger Tsien, was the first widely used ratiometric probe for biomolecule sensing (150). Ratiometric fluorescent probes show a shift in their excitation or emission spectra on reaction with their corresponding analytes. This feature is highly desirable in live cell imaging because it provides an internal standard that allows for the correction of artifacts due to photobleaching, variations in laser intensity, and inhomogeneous probe concentration inside cells. Figure 3 explains the chemical principle behind the ratiometric measurements and the strategy to quantify analyte under different scenarios. At equilibrium conditions, the concentration of an analyte is proportional to the ratio of reacted and unreacted probe independent of the absolute probe concentration, given that the probe concentration is much lower than that of the analyte (Eq 1, Fig. 3A).

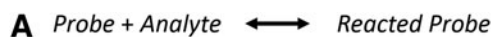
However, the quantitation equation can be complicated if there is spectral overlap or if the concentrations of analyte and probe are similar (Eq 2, Fig. 3A) (67). When there is no spectral overlap between reacted and unreacted probes, the analyte concentration is proportional to the ratio  $R$  between reacted and unreacted probes (Eq 3, Fig. 3A). It should be noted that all these calculations are based on the prerequisite that a *chemical equilibrium* is established between the analyte and the probe. Therefore, irreversible reaction-based probes are unsuitable for ratiometric-based quantitative measurements.

#### Wavelengths of fluorescent probes

When designing fluorescent probes for biological applications, it is important to consider appropriate excitation and emission wavelengths. Although some commercially available plate readers have light sources with tunable wavelengths, almost all laser-based instruments can only accommodate very limited excitation wavelengths. Commercially available laser sources usually cover 405, 488, 514, 543, 594, and 633 nm, with some high-end products also including 355, 441, 458, 532, 561, 611, 647, and 694 nm excitation wavelengths. Due to budget concerns, most instruments are equipped with no more than five laser sources at the same time. The efficiency of excitation decreases significantly when the excitation laser does not match the absorption maximum of a fluorophore.

Moreover, when a fluorophore has an excitation spectrum in between two laser wavelengths, it may create severe leaking artifacts, interfering with both channels simultaneously. The same concerns apply to emission wavelengths, although some instruments allow tunable emission bands. When designing probes, it is important to use fluorophores with appropriate excitation and emission spectra to minimize potential cross-talk between different fluorescence channels.

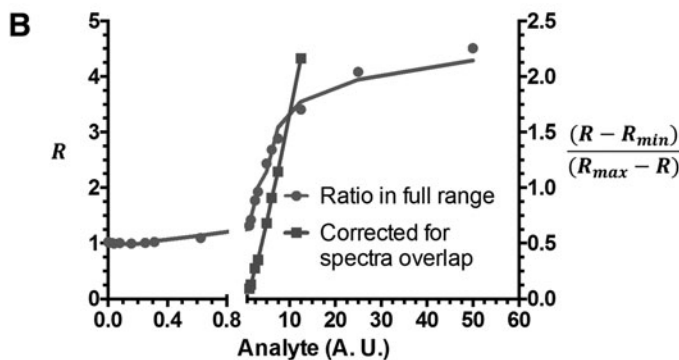
Developing a set of probes with different excitation wavelengths is advantageous due to the potential for multiplexing with other fluorescent probes or stains. For example, taking advantage of  $\text{H}_2\text{O}_2$ -responsive boronate chemistry, a series of  $\text{H}_2\text{O}_2$  probes were developed based on fluorescein, rhodamine, and several other fluorophores (14, 163). These



$$[\text{Analyte}] = K \frac{[\text{Reacted Probe}]}{[\text{Probe}]} \quad (\text{Eq 1}) \quad K \text{ is the dissociation equilibrium constant}$$

$$[\text{Analyte}] = K' \frac{(R - R_{\min})}{(R_{\max} - R)} \quad (\text{Eq 2}) \quad \text{When spectra overlap between probe and reacted probe}$$

$$[\text{Analyte}] = K'' \times R \quad (\text{Eq 3}) \quad \text{When no spectra overlap between probe and reacted probe}$$



**FIG. 3. Equations for quantification of analyte concentration using ratiometric probes in different scenarios.** (A) Equation 1 defines the relationship between the concentrations of analyte, probe, and reacted probe and the dissociation equilibrium constant  $K$ . Equation 2 is used when there is spectral overlap between the unreacted probe and the reacted probe.  $R$  is the signal ratio between reacted probe and unreacted probe.  $R_{\min}$  and  $R_{\max}$  are the  $R$  values at the corresponding 0 and saturated analyte concentrations. Equation 3 is used when there is no spectral overlap between the probe and the reacted probe. (B) The relationship between  $R$  and a hypothetical analyte concentration. In general, plotting  $R$  versus analyte concentration affords a sigmoidal relationship. In contrast,  $(R - R_{\min})/(R_{\max} - R)$  is linear when plotted against the analyte concentration.

probes were multiplexed with a pH-sensitive probe to detect  $\text{H}_2\text{O}_2$  under various pH conditions, as well as with an  $\text{HClO}$  probe to simultaneously detect  $\text{HClO}$  and  $\text{H}_2\text{O}_2$  in live cells (36, 140).

Near-infrared (NIR) fluorophores gained special attention due to their potential *in vivo* applications and low phototoxicity (78, 169, 170, 181). As Wäldchen *et al.* pointed out, phototoxicity decreases exponentially when wavelength increases (157). NIR lasers also have excellent tissue penetration ability. Several cyanine-based  $\text{H}_2\text{O}_2$  probes have been shown to be useful for *in vivo* applications (72, 120, 123). Silicon-rhodamine-based fluorophores, developed by the Nagano group, recently emerged as a new class of high quantum yield NIR fluorophores (80).  $\text{H}_2\text{O}_2$  probes based on this class of fluorophore have also been reported (187).

### Overcoming Cellular Barriers

#### *Solubility and membrane permeability of probes*

The intracellular environment is far more complicated than a homogenous mixture of proteins and small molecules, but it is spatially organized. The overall concentration of proteins can be as high as 5 mM, but these proteins are neither randomly nor evenly distributed inside cells. Instead, there are many organelles or compartments separated by lipid bilayers, creating hydrophilic pockets with hydrophobic boundaries. Therefore, the solubility of probe molecules can bias their localization and sometimes fluorescence properties as well.

For example, a hydrophobic fluorescent probe tends to show higher fluorescence readouts in lipid membranes than

in the cytosol due to its preferential accumulation in hydrophobic environments. However, this does not necessarily mean that the analyte concentration is higher in membranes than in the cytosol. Therefore, to detect hydrophilic analytes, probes should have sufficient aqueous solubility to avoid potential artifacts. LogP values, which measure the partition of a molecule in an octanol-water biphasic system, are commonly used in medicinal chemistry to evaluate the solubility of drug molecules. We recommend integrating LogP measurements in the development of probes to ensure sufficient aqueous solubility.

Typical methods for increasing water solubility include adding carboxylic acid groups, hydroxyl groups, or other hydrophilic groups to the probe core structure. However, these functional groups are usually very polar, making it difficult for the probe to cross the hydrophobic plasma membrane. Several strategies have been developed to tackle this problem. The most well-known method is replacing the carboxylic acid groups with acetylmethoxyl (AM) esters, which are hydrophobic enough to cross the plasma membrane but cleavable by intracellular esterases so that the acid form of the parent probe is regenerated once inside the cell (69, 147, 149). In addition, the acid form of probes is usually cell impermeable, which prevents the probe from leaking out of the cells once it has been internalized.

The AM ester strategy has been applied in many redox probes. It should be noted that the hydrolysis of AM esters releases formaldehyde, which may cause toxicity and/or alter the cellular redox state. Lowering the probe loading concentration can help to reduce the impact of the probe on cells.



### Protein interference with sensing reactions

ROS/RNS are highly reactive small molecules, and their concentrations are tightly regulated in cells by a number of redox-active enzymes. To detect ROS/RNS, probe molecules must react quickly enough with ROS/RNS to compete with highly efficient ROS/RNS scavenging enzymes. For example, it has been reported that the most popular boronate ester sensing group for H<sub>2</sub>O<sub>2</sub> can be outcompeted kinetically by proteins, such as glutathione peroxidases (GPx) and catalase (70). Therefore, the signal from these fluorescent probes only represents a small portion of the intracellular H<sub>2</sub>O<sub>2</sub> pool.

In fact, most reported boronate ester-based H<sub>2</sub>O<sub>2</sub> probes can only be used to measure increases in H<sub>2</sub>O<sub>2</sub> concentrations in the micromolar range either from bolus administration of external ROS or under very special biological events, such as immune responses (36). To the best of our knowledge, we are unaware of anyone successfully using small-molecule fluorescent probes to measure physiologically relevant concentrations of H<sub>2</sub>O<sub>2</sub> in cells.

In the development of glutathione probes, the highly abundant protein thiols could also react with the probes. To test this possibility, our group developed a GPC-based method with fluorescence detection to assess protein interactions with small-molecule GSH probes (67). This method could be modified and adapted to the development of other redox probes.

### Probe turnover and clearance in live cells

Fluorescent probes are essentially xenobiotics to cells. Cells actively clear these xenobiotics through various mechanisms, including inactivation by P450 enzymes and excretion through ATP-binding cassette (ABC) transporters (65). Therefore, for live cell experiments, researchers need to take the intracellular turnover of probe molecules into consideration, preferably

measuring the half-life of probe clearance. In the event of rapid probe clearance, time-lapsed experiments with relatively long incubation times may not be feasible. To address this problem, one could try to use ABC transporter inhibitors, such as probenecid, to reduce probe clearance (155, 156). If the clearance mechanism is unclear or the clearance rate cannot be reduced to the desired extent, the best approach would be to prepare a series of samples at different time points and stain each sample individually by using exactly the same conditions.

Designing experiments to perform quantitative detection of redox signaling molecules in live cells can be complicated and requires a number of controls; however, live cell experiments provide much more physiologically relevant information than bulk measurements using lysates.

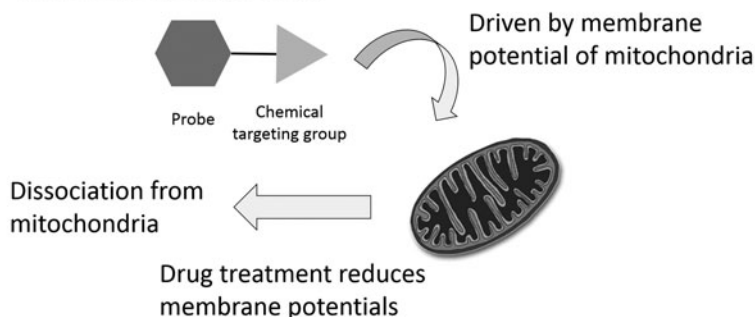
### Organelle specificity of small-molecule probes

The subcellular dynamics of redox signaling molecules have gained increasing attention in recent years. Redox probes targeting mitochondria (34, 41, 97, 107, 115, 162, 171), lysosome (76, 100, 124, 187), nucleus (37, 161), endoplasmic reticulum (7, 167), and plasma membrane (77) have all been reported.

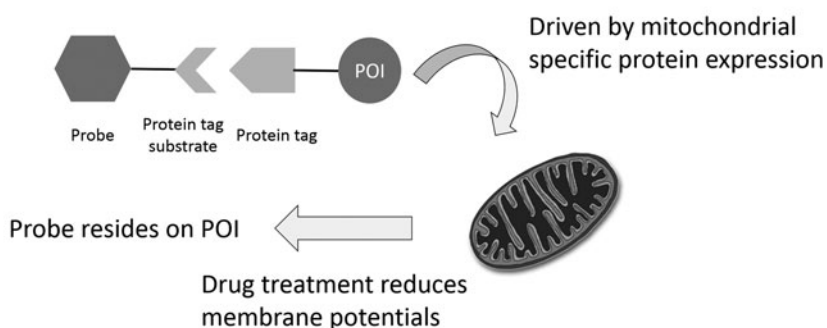
For example, the triphenylphosphonium (TPP) group is commonly used in probe design for mitochondrial targeting, taking advantage of the highly negative mitochondrial membrane potential (Fig. 4A) (17). Probes with this group have been used to demonstrate how treatments with drugs, such as rotenone or antimycin A, can reduce the mitochondrial membrane potential. However, the reduction in fluorescence observed during these experiments could have been due to the probe dissociating from the mitochondria rather than from an actual decrease in the analyte concentration. Therefore, one must be very careful when interpreting the results of studies done with organelle-specific probes.

**FIG. 4. Two strategies for achieving organelle specificity for small-molecule fluorescent probes.** (A) Chemical targeting strategy. A chemical targeting group, such as TPP for mitochondria targeting, can be conjugated with the probe. The accumulation of the probe-TPP conjugate in mitochondria is driven by the negative mitochondrial membrane potential. (B) Protein tag targeting strategy. This is a two-step strategy. Protein tagging systems, such as Halo and SNAP, can be fused with a POI that is specifically expressed in certain organelles. Then, a conjugate between the probe and the protein tag substrate will react with the organelle-specific protein tag to achieve organelle specificity. TPP, triphenylphosphonium; POI, protein-of-interest.

#### A Chemical targeting strategy



#### B Protein tag targeting strategy



Protein tagging technologies, such as Halo-Tag (18, 102), SNAP-Tag (1, 50, 75, 113, 127), CLIP-Tag (50), and ACP-Tag (51, 177), can provide an alternative strategy for organelle targeting. Many small-molecule organelle targeting groups are synthetically difficult to produce, whereas protein tags are synthetically convenient and expandable to essentially all subcellular targets (Fig. 4B). For example, the Halo-tag protein can be fused with a nuclear-specific protein or nuclear localization sequence to specifically express the Halo-tag protein in the nucleus. Small-molecule probes can then be conjugated with the Halo-tag substrate to specifically react with the Halo-tag protein expressed in a particular organelle.

Although this method does require transfection of cells, similar to genetically encoded probes, this hybrid strategy provides a nice general method for positioning small-molecule probes in cells with subcellular resolution.

### Small-Molecule Fluorescent Probes for Redox Signaling

To better assist readers in assessing the performance of redox-active fluorescent probes using the concepts of probe design, here we provide a brief summary of some of the representative probes and categorize them by their sensing reactions. We also excerpt available data including reaction selectivity, typical staining concentration, reaction kinetics, and wavelengths from these reports. Comprehensive summaries of more recently developed redox fluorescent probes can be found in these review articles (8, 14, 21, 22, 24, 55, 87, 92, 103, 111, 144, 145, 166, 183).

#### *H<sub>2</sub>O<sub>2</sub>-responsive probes*

$H_2O_2$ -responsive probes are categorized into five groups: boronate-based probes (the most popular option), benzil-based probes, chalcogenides-based probes, metal-mediated probes, and other probes (Table 1).

As mentioned earlier, boronate-based hydrogen peroxide probes have good selectivity toward  $H_2O_2$  at micromolar concentration levels (15, 25, 86, 98, 100, 116, 171, 189). The cross-reactivity is typically tested in a test tube experiment against a panel of individual ROS/RNS. The typical staining concentration used for cell experiments is in the low micromolar range, with the exception of the AIE-based probe that requires a staining concentration as high as 1 mM (189). To detect an increase of  $H_2O_2$  of  $\sim 100 \mu M$ , the typical incubation time for these probes is 30 min. Peroxyfluor-1 (PF1) only requires a 5-min incubation due to its fast reaction with  $H_2O_2$  (15). For benzil-based probes, the reaction kinetics are generally faster than for boronate-based probes. An incubation time of only 10 min is needed before reading the signal (1, 2).

Testing of cross-reactivity between benzil-based probes and other ROS/RNS is performed in the same manner as that of boronate-based probes, and the results are similar. Chalcogenide-based probes take advantage of the affinity between oxygen and chalcogenide atoms, as well as the reversibility of such oxidation reactions. However, the selectivity profile for this kind of probe is not well established. To date, these probes seem to be more suitable as overall redox state probes instead of  $H_2O_2$ -selective probes. More detailed data from biological studies are required before we can fully assess their performance (74, 78).

Metal-mediated probes mainly rely on transition metals and their affinity toward oxygen under specific conditions. Few

probes of this type have been reported, and there are few, if any, common properties within the group (62, 139). Other probes include the first  $H_2O_2$ -cleavable sulfonate probe (106) and the phenol oxidation-based probe (180). The common properties of hydrogen peroxide-responsive probes are summarized in Table 2.

#### *Peroxynitrite-responsive probes*

Peroxynitrite-responsive probes are categorized into three main groups: addition-based probes, oxidation-based probes, and other probes (Table 3). One type of addition-based probe relies on the addition of the NO moiety onto a secondary acyl amine (91, 109). Another type relies on the electrophilic addition of the whole molecule onto a positively charged acceptor (27, 192). Both types of addition-based probes showed good selectivity among a panel of ROS/RNS in *in vitro* experiments; however, the experiments were not performed by using physiologically relevant concentrations of all ROS/RNS. Specifically, the ONOO<sup>-</sup> was tested at a concentration of 10  $\mu M$  or higher, which is hundreds of folds higher than its physiological concentration. These probes are administered to cells at low micromolar concentrations and require 20–30 min of incubation before acquiring signals.

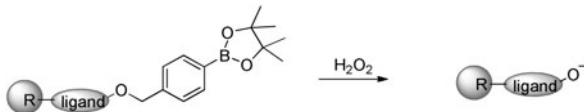
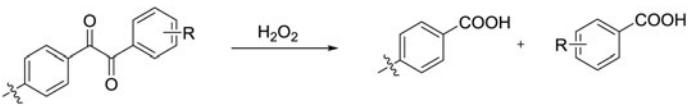
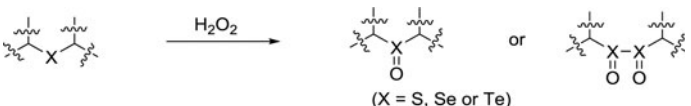
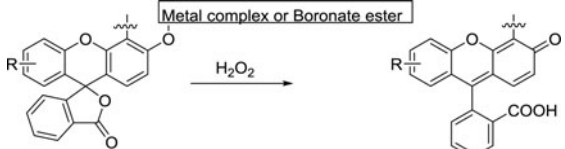
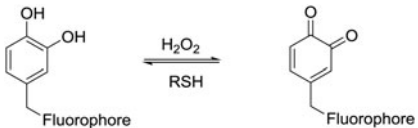
The last type of addition-based probes has a special design that incorporates an addition reaction with a cyclization step (142, 173). The authors claim that such a reaction design significantly improved selectivity, especially against hydrogen peroxide. However, because the physiologically relevant concentration of ONOO<sup>-</sup> is significantly lower than that of  $H_2O_2$ , selective detection of ONOO<sup>-</sup> is still challenging in cells. Even using these probes, the authors observed that signals generated from probes reacting with ONOO<sup>-</sup> were at most  $\sim 200$ -fold higher than those generated by other ROS/RNS if all of them are at a similar concentration level. Considering the physiologically relevant concentration differences, at least 50% of their signal may come from nonspecific reactions between probes and other ROS/RNS inside a cell.

Oxidation-based probes can be further divided into three groups, phenol-based (88, 122), boronate-based (141, 182), and Te-based (181) probes. As mentioned earlier, most phenol-based and Te-based probes are best used as indicators of the overall redox state. However, some *in vitro* experiments reveal excellent selectivity between ONOO<sup>-</sup> and other ROS/RNS, with a difference in response of up to several thousand folds. This is potentially due to a kinetic difference (122). Boronate-based probes react with ONOO<sup>-</sup> quickly, but due to the low concentration of ONOO<sup>-</sup> inside cells, they still require a 30-min incubation time before optimal signals can be detected (84, 128, 141, 182). There are also a few other interesting mechanisms that have been applied to ONOO<sup>-</sup> sensing (13). The available common properties of peroxynitrite-responsive probes are summarized in Table 3.

#### *HCIO-responsive probes*

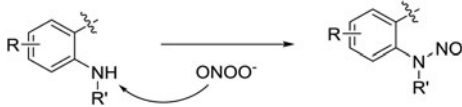
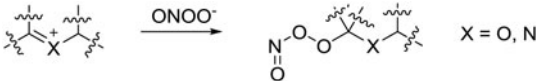
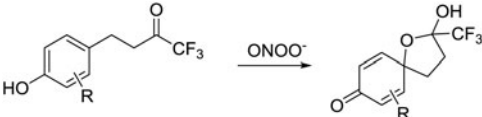
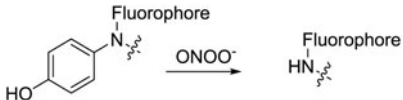
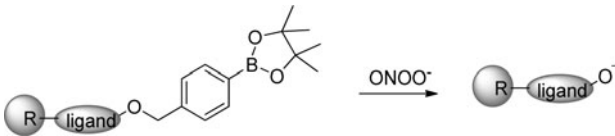
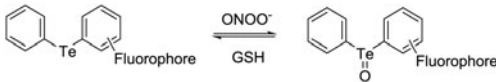
HCIO-responsive probes are all oxidation-based probes, and they are categorized into three sub-types (Table 4): chalcogenides-based (104, 154, 184), phenol/aniline-based (64, 81, 193), and thiol ether-based probes (11, 79). These oxidation-based probes, regardless of reaction reversibility, are mostly overall redox state indicators. The selectivity tests for these probes are usually performed by comparing probe responses with micromolar concentrations of all ROS/RNS

TABLE 2. H<sub>2</sub>O<sub>2</sub>-RESPONSIVE PROBES

Name	Species tested for cross-reactivity	Reported staining concentration for cells	Time needed before optimal signal available	$\lambda_{ex}/\lambda_{em}$ (nm)	References
<b>Boronate-based probes</b>					
					
PAM-BN-PB	CH <sub>3</sub> COOH, TBHP, ClO <sup>-</sup> , O <sub>2</sub> <sup>·-</sup> , ·OH, <sup>-</sup> OtBu, GSH, Vc, ONOO <sup>-</sup> , H <sub>2</sub> O <sub>2</sub>	10 $\mu$ M	30–60 min	410/480	(25)
HP-L1	K <sup>+</sup> , Na <sup>+</sup> , Ca <sup>2+</sup> , Mg <sup>2+</sup> , Zn <sup>+</sup> , Cu <sup>2+</sup> , Fe <sup>2+</sup> , GSH, Cys, HClO, H <sub>2</sub> O <sub>2</sub>	5 $\mu$ M	30 min	520/584	(100)
Mito-H <sub>2</sub> O <sub>2</sub>	HClO, O <sub>2</sub> <sup>·-</sup> , <sup>-</sup> OtBu, ·OH, TBHP, NO, ONOO <sup>-</sup> , GSH, Vc, Glu, HSO <sub>3</sub> <sup>-</sup> , H <sub>2</sub> O <sub>2</sub>	10 $\mu$ M	30–90 min	490/527	(171)
QCy-BA	OCI <sup>-</sup> , O <sub>2</sub> <sup>·-</sup> , TBHP, ·OH, <sup>-</sup> OtBu, NO, ONOO <sup>-</sup> , H <sub>2</sub> O <sub>2</sub>	5 $\mu$ M	30 min	400/565–680	(116)
PF1	OCI <sup>-</sup> , O <sub>2</sub> <sup>·-</sup> , TBHP, ·OH, <sup>-</sup> OtBu, NO, H <sub>2</sub> O <sub>2</sub>	5 $\mu$ M	5 min	450/460–700	(15)
TPE-DABA (AIE)	OCI <sup>-</sup> , O <sub>2</sub> <sup>·-</sup> , TBHP, ·OH, <sup>-</sup> OtBu, NO, NO <sub>3</sub> <sup>-</sup> , ONOO <sup>-</sup> , H <sub>2</sub> O <sub>2</sub>	50 $\mu$ M	N/A	430/576	(98)
TPE-BO (AIE)	<sup>1</sup> O <sub>2</sub> , NO, ClO <sup>-</sup> , TBHP, ·OH, O <sub>2</sub> <sup>·-</sup> , GSH, H <sub>2</sub> O <sub>2</sub>	5 $\mu$ M to 1.0 mM	N/A	400/500	(189)
D-BBO (AIE)	<sup>1</sup> O <sub>2</sub> , NO, ClO <sup>-</sup> , TBHP, ·OH, O <sub>2</sub> <sup>·-</sup> , H <sub>2</sub> O <sub>2</sub>	N/A	N/A	405/510	(86)
<b>Benzil-based probes</b>					
					
NBzF-BG	N/A	2 $\mu$ M	10 min	505/525	(1)
NBzF	<sup>1</sup> O <sub>2</sub> , ONOO <sup>-</sup> , NO, ClO <sup>-</sup> , TBHP, ·OH, O <sub>2</sub> <sup>·-</sup> , H <sub>2</sub> O <sub>2</sub>	5 $\mu$ M	10 min	495/519	(2)
<b>Chalcogenides-based probes</b>					
					
2-Me TeR	ONOO <sup>-</sup> , NO, ClO <sup>-</sup> , ·OH, O <sub>2</sub> <sup>·-</sup> , H <sub>2</sub> O <sub>2</sub>	5 $\mu$ M	N/A (short lived)	660/690	(78)
Compound 3	N/A	N/A	N/A	500/565	(74)
<b>Metal-mediated redox probes</b>					
					
ZP1Fe <sub>2</sub>	CAN, DDQ, ClO <sup>-</sup> , O <sub>2</sub> <sup>·-</sup> , <sup>-</sup> OtBu, ·OH, TBHP, NO, H <sub>2</sub> O <sub>2</sub>	10 $\mu$ M	30 min	507/533	(139)
MBFh1	N/A	5 $\mu$ M	1 min	570/590	(62)
Other probes					
1a	ONOO <sup>-</sup> , NO, TBHP, ClO <sup>-</sup> , ·OH, O <sub>2</sub> <sup>·-</sup> , O <sub>2</sub> <sup>·-</sup> +catayse, O <sub>2</sub> <sup>·-</sup> +SOD, H <sub>2</sub> O <sub>2</sub>	25 $\mu$ M	60 min	485/530	(106)
					
DA-Cy	·OH, MeLOOH, CuOOH, tBuOOH, O <sub>2</sub> <sup>·-</sup> , <sup>1</sup> O <sub>2</sub> , ClO, H <sub>2</sub> O <sub>2</sub>	5 $\mu$ M	3 min	630/755	(180)

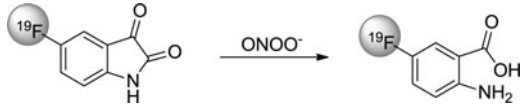
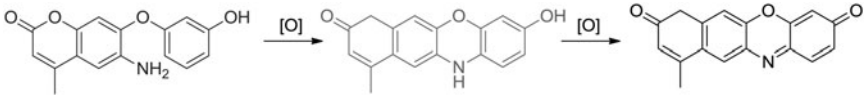
AIE, aggregation induced emission; N/A, not available; NO, nitric oxide; O<sub>2</sub><sup>·-</sup>, superoxide; OCI<sup>-</sup>, hypochlorite; OH·, hydroxyl radical; ONOO<sup>-</sup>, peroxyntirite.

TABLE 3. PEROXYNITRITE-RESPONSIVE PROBES

Name	Species Tested for Cross-Reactivity	Reported Staining Concentration for Cells	Time Needed before Optimal Signal Available	$\lambda_{ex}/\lambda_{em}$ (nm)	References
<i>Addition-based probes</i>					
					
A2	$\text{OCl}^-$ , $\text{O}_2^{\cdot-}$ , $\cdot\text{OH}$ , $\text{ROO}^-$ , $\text{NO}$ , $\text{ONOO}^-$ , $\text{H}_2\text{O}_2$ , $\text{NO}_2^-$ , $^1\text{O}_2$	2 $\mu\text{M}$	20 min	485/517	(109)
Ds-DAB	$\text{OCl}^-$ , $\text{O}_2^{\cdot-}$ , $\cdot\text{OH}$ , $\text{NO}$ , $\text{NO}_3^-$ , $\text{ONOO}^-$ , $\text{H}_2\text{O}_2$ , $\text{NO}_2^-$ , $\text{HNO}$	10 $\mu\text{M}$	30 min	350/505	(91)
					
MITO-CC	$\text{OCl}^-$ , $\text{O}_2^{\cdot-}$ , $\cdot\text{OH}$ , $\text{NO}$ , $\text{NO}_3^-$ , $\text{ONOO}^-$ , $\text{H}_2\text{O}_2$ , $\text{NO}_2^-$ , TBHP, $\text{BuO}\cdot$ , $\text{H}_2\text{S}$ , $\text{H}_2\text{S}_2$ , $\text{SO}_3^{2-}$ , $\text{HNO}$	5 $\mu\text{M}$	20 min	420/651	(27)
CHCN	$\text{OCl}^-$ , $\text{O}_2^{\cdot-}$ , $\cdot\text{OH}$ , $\text{ROO}^-$ , $\text{NO}$ , $\text{ONOO}^-$ , $\text{H}_2\text{O}_2$ , Cys, Hcy, GSH, TBHP	5 $\mu\text{M}$	30 min	515/635	(192)
					
HKGreen-1	$\text{OCl}^-$ , $\text{O}_2^{\cdot-}$ , $\cdot\text{OH}$ , $\text{ROO}^-$ , $\text{NO}$ , $\text{ONOO}^-$ , $\text{H}_2\text{O}_2$ , $^1\text{O}_2$	20 $\mu\text{M}$	15 min	490/521	(173)
HKGreen-2	$\text{OCl}^-$ , $\text{O}_2^{\cdot-}$ , $\cdot\text{OH}$ , $\text{ROO}^-$ , $\text{NO}$ , $\text{ONOO}^-$ , $\text{H}_2\text{O}_2$ , $^1\text{O}_2$ , $\text{NO}$ , $\text{NO}_3^-$	20 $\mu\text{M}$	60 min	520/539	(142)
<i>Oxidation-based probes</i>					
					
HKGreen-4	$\text{OCl}^-$ , $\text{O}_2^{\cdot-}$ , $\cdot\text{OH}$ , $\text{ROO}^-$ , $\text{NO}$ , $\text{ONOO}^-$ , $\text{H}_2\text{O}_2$ , $^1\text{O}_2$	10 $\mu\text{M}$	60 min	517/535	(122)
NP3 (ESIPT)	$\text{OCl}^-$ , $\text{O}_2^{\cdot-}$ , $\cdot\text{OH}$ , $\text{ROO}^-$ , $\text{NO}$ , $\text{ONOO}^-$ , $\text{H}_2\text{O}_2$ , $^1\text{O}_2$ , Ala, Gly, Cys, GSH, $\text{Cu}^{2+}$ , $\text{Fe}^{2+}$ , $\text{Fe}^{3+}$ , $\text{Zn}^{2+}$	5 $\mu\text{M}$	30 min	405/420–480	(88)
					
1-D-fructose	$\text{OCl}^-$ , $\text{O}_2^{\cdot-}$ , $\cdot\text{OH}$ , $\text{ROO}^-$ , $\text{NO}$ , $\text{NO}_3^-$ , $\text{ONOO}^-$ , $\text{H}_2\text{O}_2$ , $\text{NO}_2^-$	5 $\mu\text{M}$	30 min	410/525	(141)
PyBor	$\text{OCl}^-$ , $\text{O}_2^{\cdot-}$ , $\cdot\text{OH}$ , $\text{NO}$ , $\text{ONOO}^-$ , $\text{H}_2\text{O}_2$ , TBHP, $\text{CuOOH}$ , $\text{BrO}$	10 $\mu\text{M}$	30 min	347/410	(182)
Fl-B	N/A	50 $\mu\text{M}$	30 min	492/515	(128)
					
Cy-NTe	$\text{OCl}^-$ , $\text{O}_2^{\cdot-}$ , $\cdot\text{OH}$ , $\text{NO}$ , $\text{ONOO}^-$ , $\text{H}_2\text{O}_2$ , TBHP, $\text{CuOOH}$ , $\text{MeLOOH}$	1 $\mu\text{M}$	5 min	793/820	(181)

(continued)

TABLE 3. (CONTINUED)

Name	Species Tested for Cross-Reactivity	Reported Staining Concentration for Cells	Time Needed before Optimal Signal Available	$\lambda_{ex}/\lambda_{em}$ (nm)	References
Other probes					
					
5-Fluoroisatin		Detected by $^{19}\text{F}$ NMR			(13)
					
PN <sub>600</sub>		Three-channel fluorescent probe			(188)

Cys, cysteine; ESIPT, excited state intramolecular proton transfer;  $^1\text{O}_2$ , singlet oxygen.

including HClO, which do not represent their corresponding physiologically relevant concentrations. The staining concentration is usually in the low micromolar range, and the typical incubation time is 15–30 min. The available common properties of HClO-responsive probes are summarized in Table 4.

#### Thiol-responsive probes

Thiol-responsive probes are categorized into two main types: reversible and irreversible reaction-based probes

(Table 5). The reversible probes are based on either Michael addition reactions or nucleophilic addition to rhodamines; whereas irreversible probes use several different reactions, including addition and substitution reactions.

A reversible Michael addition with a proper equilibrium constant can be applied to quantitative monitoring of glutathione concentrations in live cells. Since our group first introduced the concept by designing ThiolQuant-Green 2 years ago (67), several groups including our own have followed up and designed probes with improved reaction kinetics (16, 66,

TABLE 4. HClO-RESPONSIVE PROBES

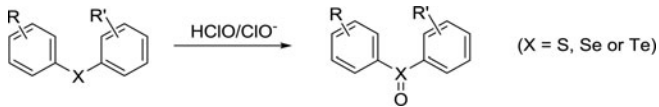
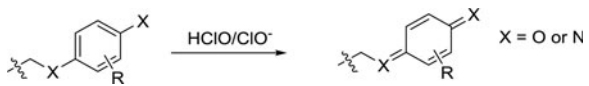
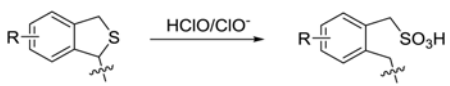
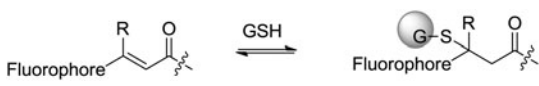
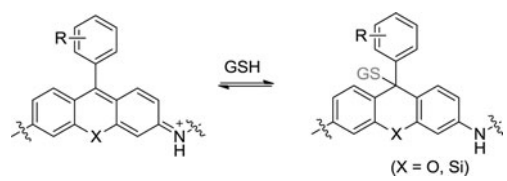
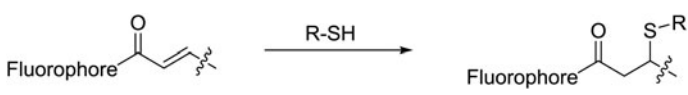
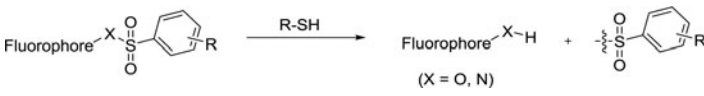
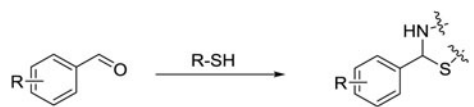
Name	Species tested for cross-reactivity	Reported staining concentration for cells	Time needed before optimal signal available	$\lambda_{ex}/\lambda_{em}$ (nm)	References
					
Mito-TP	$\text{OCl}^-$ , $\text{O}_2^{\cdot-}$ , $\cdot\text{OH}$ , NO, $\text{ONOO}^-$ , $\text{H}_2\text{O}_2$ , TBHP, $\text{BuO}\cdot$ , $\text{NO}\cdot$ , $\text{tBuOO}\cdot$ , ATP, ADP, NAD, GSH, Cys, $\text{Fe}^{3+}$ , $\text{Zn}^{2+}$ , $\text{Cu}^{2+}$ ,	10 $\mu\text{M}$	20 min	375/500	(184)
NI-Se	$\text{OCl}^-$ , $\text{O}_2^{\cdot-}$ , $\cdot\text{OH}$ , NO, $\text{ONOO}^-$ , $\text{H}_2\text{O}_2$ , TBHP, $^1\text{O}_2$ , CHP	10 $\mu\text{M}$	5 min	488/490–590	(104)
HCTe	$\text{OCl}^-$ , $\text{O}_2^{\cdot-}$ , $\cdot\text{OH}$ , NO, $\text{NO}_3^-$ , $\text{ONOO}^-$ , $\text{H}_2\text{O}_2$ , $\text{NO}_2^-$ , TBHP, $^1\text{O}_2$	10 $\mu\text{M}$	30 min	480/531	(154)
					
BClO	$\text{OCl}^-$ , $\text{O}_2^{\cdot-}$ , $\cdot\text{OH}$ , NO, $\text{H}_2\text{O}_2$ , TBHP, $\text{tBuO}\cdot$ , $^1\text{O}_2$	1 $\mu\text{M}$	20 min	480/505	(193)
HKOCl-2	$\text{OCl}^-$ , $\text{O}_2^{\cdot-}$ , $\cdot\text{OH}$ , NO, $\text{H}_2\text{O}_2$ , TBHP, $\text{ONOO}^-$ , $\text{ROO}\cdot$ , $^1\text{O}_2$	10 $\mu\text{M}$	30 min	523/545	(64)
MitoAR	$\text{OCl}^-$ , $\text{O}_2^{\cdot-}$ , $\cdot\text{OH}$ , $\cdot\text{NO}$ , $\text{H}_2\text{O}_2$ , $\text{ONOO}^-$	1 $\mu\text{M}$	15 min	543/560	(81)
					
Hypo-SiF	$\text{OCl}^-$ , $\text{KO}_2$ , $\cdot\text{OH}$ , $\cdot\text{NO}$ , $\text{H}_2\text{O}_2$ , $\text{ONOO}^-$	N/A	N/A	570/606	(11)
MMSiR	$\text{OCl}^-$ , $\text{KO}_2$ , $\text{O}_2^{\cdot-}$ , $\cdot\text{NO}$ , $\text{H}_2\text{O}_2$ , $\text{ONOO}^-$	1 $\mu\text{M}$	4 min	620/670	(79)

TABLE 5. THIOL-RESPONSIVE PROBES


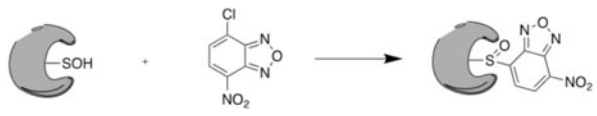

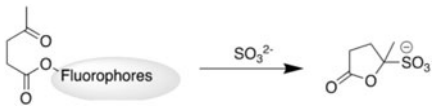
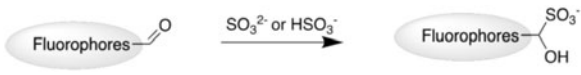
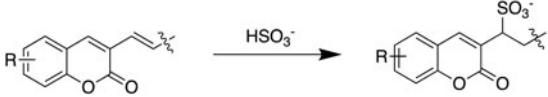
Name	Species tested for cross-reactivity	Reported staining concentration for cells	Time needed before optimal signal available	$\lambda_{ex}/\lambda_{em}$ (nm)	References
Reversible reaction-based probes					
					
RealThiol	GSH, Gly, Lysate, Cys, H <sub>2</sub> S, Lipoic acid, KSCN, Na <sub>2</sub> S <sub>2</sub> O <sub>3</sub> , NO, H <sub>2</sub> O <sub>2</sub> , HOCl, O <sub>2</sub> <sup>-</sup> , NaNO <sub>2</sub> , Protein thiols	0.1–1 $\mu$ M	1–5 min	405/487 488/565	(66)
TQ-Green	GSH, Cys, BSA, Lysate	1 $\mu$ M	15–30 min	405/488 488/565	(67)
QG-1	H <sub>2</sub> O <sub>2</sub> , GSH	10 $\mu$ M	1 min	405/488 488/560	(101)
					
QG3.0	H <sub>2</sub> O <sub>2</sub> , GSH	1 $\mu$ M	1–5 min	558/593 609/632	(151)
Irreversible reaction-based probes					
					
Probe 1	Glu, Ala, Arg, Val, Ser, Lys, Leu, Adenine, Guanine, Cytosine, Thymine, Glucose, Ca <sup>2+</sup> , Mg <sup>2+</sup> , K <sup>+</sup> , Na <sup>+</sup> , Zn <sup>2+</sup> , Fe <sup>3+</sup> , NADH, H <sub>2</sub> O <sub>2</sub>	N/A	N/A	444/496	(93)
1	Ca <sup>2+</sup> , Mg <sup>2+</sup> , K <sup>+</sup> , Na <sup>+</sup> , Zn <sup>2+</sup> , Fe <sup>3+</sup> , Cu <sup>2+</sup> , Hg <sup>2+</sup> , GSH	1 $\mu$ M	5 min	400/420–600	(175)
					
Probe	DTT, 3'-thio dT, Glu, Ala, Arg, Lys, ME, Vc, H <sub>2</sub> O <sub>2</sub>	25 $\mu$ M	15 min	490/522	(135)
					
Aldehyde 1	Glu, Ala, Arg, Ser, Lys, Leu, Pro, His, Gln, GSH, Cys	N/A	N/A	315/360	(143)

101, 151). All these GSH probes have reaction kinetics in the seconds to minutes range, and they have been demonstrated to quantitatively follow GSH dynamics in living cells.

It should be noted that these probes are claimed to be selective for GSH based on the fact that GSH is the most abundant small-molecule thiol in eukaryotic cells. However, some organisms use trypanothione (45), mycothiol (118), or bacillithiol (119) instead of glutathione. In these cases, the GSH probes could be repurposed to quantify these other small-molecule thiols assuming their concentrations are in the mM range.

Despite using similar Michael addition reactions, some GSH probes with suboptimal equilibrium constants and/or sluggish reaction kinetics cannot be used for time-lapsed experiments (93, 175). When coupling two addition reactions for cyclization, several folds of selectivity between different biothiols have been achieved. However, since GSH is the dominant free thiol in cells, it is difficult to achieve selective signal detection under physiological conditions (143). The nucleophilicity of thiols has also been utilized to design substitution reaction-based thiol probes

TABLE 6. PROBES FOR OTHER REDOX METABOLITES

Name	Species tested for cross-reactivity	Reported staining concentration for cells	Time needed before optimal signal available	$\lambda_{ex}/\lambda_{em}$ (nm)	References
Sulfenic acid probes					
					
Used for labeling in cell lysates					
DAz-1	N/A	10 mM	2 h	N/A	(132)
DAz-2	N/A	5 mM	2 h	N/A	(83)
					
NBD-Cl	N/A	1 $\mu$ M	30 min	Various (absorbance at 340 nm)	(43)
Sulfane sulfur probe					
					
SSP2	Cys, GSH, Hcy, GSSG, Na <sub>2</sub> S, Na <sub>2</sub> S <sub>2</sub> O <sub>3</sub> , Na <sub>2</sub> SO <sub>3</sub> , Na <sub>2</sub> SO <sub>4</sub> , formaldehyde, acetaldehyde, Na <sub>2</sub> S <sub>2</sub> , Cys-poly-sulfide, S <sub>8</sub>	50 $\mu$ M	20 min	482/518	(20)
DSP-3	GSH, Cys, Hcy, GSSG, Na <sub>2</sub> S, Na <sub>2</sub> S <sub>2</sub> O <sub>3</sub> , Na <sub>2</sub> SO <sub>3</sub> , Na <sub>2</sub> SO <sub>4</sub> , CH <sub>3</sub> SSSCH <sub>3</sub> , S <sub>8</sub> , Na <sub>2</sub> S <sub>2</sub>	10 $\mu$ M	20 min	490/515	(95)
Sulfite and bisulfite probes					
					
Probe 1	F <sup>-</sup> , Cl <sup>-</sup> , Br <sup>-</sup> , I <sup>-</sup> , SO <sub>4</sub> <sup>2-</sup> , HPO <sub>4</sub> <sup>2-</sup> , NO <sub>3</sub> <sup>-</sup> , N <sub>3</sub> <sup>-</sup> , AcO <sup>-</sup> , ClO <sub>4</sub> <sup>-</sup> , HCO <sub>3</sub> <sup>-</sup>	N/A	N/A	487/588	(30)
					
P-1	AcO <sup>-</sup> , NO <sub>2</sub> <sup>-</sup> , NO <sub>3</sub> <sup>-</sup> , F <sup>-</sup> , CO <sub>3</sub> <sup>2-</sup> , SO <sub>4</sub> <sup>2-</sup> , Cl <sup>-</sup> , IO <sub>3</sub> <sup>-</sup> , CN <sup>-</sup> , N <sub>3</sub> <sup>-</sup> , ClO <sub>3</sub> <sup>-</sup> , Br <sup>-</sup> , SCN <sup>-</sup> , I <sup>-</sup> , HSO <sub>4</sub> <sup>-</sup> , S <sup>2-</sup> , S <sub>2</sub> O <sub>3</sub> <sup>2-</sup> , HSO <sub>3</sub> <sup>-</sup>	50 $\mu$ M	30 min	330/395–515	(29)
The probe	I <sup>-</sup> , F <sup>-</sup> , Cl <sup>-</sup> , Br <sup>-</sup> , HCO <sub>3</sub> <sup>-</sup> , SO <sub>4</sub> <sup>2-</sup> , PO <sub>4</sub> <sup>3-</sup> , NO <sub>3</sub> <sup>-</sup> , NO <sub>2</sub> <sup>-</sup> , B <sub>4</sub> O <sub>7</sub> <sup>2-</sup> , CO <sub>3</sub> <sup>2-</sup> , HPO <sub>4</sub> <sup>2-</sup> , SCN <sup>-</sup>	N/A	N/A	370/420	(178)
					
Probe 2	F <sup>-</sup> , Cl <sup>-</sup> , Br <sup>-</sup> , I <sup>-</sup> , NO <sub>2</sub> <sup>-</sup> , NO <sub>3</sub> <sup>-</sup> , N <sub>3</sub> <sup>-</sup> , OAc <sup>-</sup> , PO <sub>4</sub> <sup>3-</sup> , CO <sub>3</sub> <sup>2-</sup> , SO <sub>4</sub> <sup>2-</sup> , S <sub>2</sub> O <sub>3</sub> <sup>2-</sup> , H <sub>2</sub> O <sub>2</sub> , t-BuOOH, NaClO	10 $\mu$ M	30 min	466/523 580/663	(165)

(continued)

TABLE 6. (CONTINUED)

Name	Species tested for cross-reactivity	Reported staining concentration for cells	Time needed before optimal signal available	$\lambda_{ex}/\lambda_{em}$ (nm)	References
TSSP-N <sub>3</sub>	F <sup>-</sup> , Cl <sup>-</sup> , Br <sup>-</sup> , I <sup>-</sup> , AcO <sup>-</sup> , HCO <sub>3</sub> <sup>-</sup> , CN <sup>-</sup> , NO <sub>2</sub> <sup>-</sup> , NO <sub>3</sub> <sup>-</sup> , PO <sub>4</sub> <sup>3-</sup> , HS <sup>-</sup> , SCN <sup>-</sup> , SO <sub>4</sub> <sup>2-</sup> , S <sub>2</sub> O <sub>3</sub> <sup>2-</sup> , Cys, Hcy, GSH	5 $\mu$ M	30 min	386/460 475/590	(146)
Lipid peroxidation probes					
C11-BODIPY	N/A	1 $\mu$ M	20 min	581/595	(40)
PA derivative 1	N/A	10 $\mu$ M	30 min	405/490–520	(117)

(135). Similarly, these probes respond primarily to intracellular GSH under physiological conditions. Most of these probes are administered to cells at low micromolar concentrations. The available common properties for glutathione probes are summarized in Table 5.

#### Probes for other redox metabolites

Biochemical redox reactions involve more than just the molecules stated earlier. Continuous efforts have been made to discover other important redox signaling molecules involved in cellular metabolic; some examples include intermediates such as sulfenic acid, sulfane sulfur, sulfite, bisulfite, and peroxidized lipids. We have summarized some of the recently developed probes for these metabolic intermediates (Table 6).

When thiols are biologically modified in cells, they could go through several intermediates such as sulfenic acid, sulfane sulfur, sulfite, or bisulfite. These intermediates serve different roles in cells and are important in redox biology (57). The Carroll group has developed a series of probes targeting mostly sulfenic acid modifications on protein thiols (57–59, 83, 121, 132). These sensing reactions are mostly based on selective addition of sulfenic acid onto a metacyclohexanedione. They have been used for labeling of sulfenic acid modified proteins from cell lysate but have relatively limited applications as live cell probes.

The thiol derivatization agent, 4-chloro-7-nitrobenzofurazan, widely used in HPLC is also used as a sulfenic acid probe (43). Due to the lack of cross-reactivity tests and relatively slow kinetics, all the sensing reactions mentioned earlier are geared toward lysate-based measurements.

There are also a number of sensors developed for polysulfides, including sulfane sulfur initially used by the Xian group. They first utilized a biotin switch assay to distinguish hydrodisulfides from the predominant RSH in cell lysates (186). The same group has also developed several probes for detecting different polysulfides in live cells (20, 95, 96).

A few probes for sulfite and bisulfite have also been developed based on the reductive addition of sulfite/bisulfite onto ketones or aldehydes (29, 30, 146, 165, 178). The role of such metabolites in redox biology is not yet well established, and the physiologically relevant concentration is unknown. Therefore, it is currently difficult to predict which attributes are important in designing probes for sulfite and bisulfite.

Other important redox intermediates include oxidized lipids, oxidized protein/peptide thiols, and oxidized sugar. However, there are no small-molecule probes that can se-

lectively and reliably measure these peroxides potentially due to difficulty in sensing reaction design. There are a few reported probes for lipid peroxidation, but their cross-reactivity and bioavailability is not well studied (40, 117). More work needs to be done to demonstrate their applicability for studying redox biology.

#### Conclusions

Currently, the development of redox-responsive small-molecule fluorescent probes is primarily driven by chemists who sometimes fail to sufficiently test their probes in complex biological systems. Although many probes with new reaction centers have been reported, only a few have been tested and applied by redox biologists. There is an urgent need to strengthen the communication between probe developers, mostly chemists, and redox biologists.

The most challenging questions for developing new redox probes are: (i) how to develop new sensing reactions that target different analytes, (ii) how to optimize these probes for real-time quantitation in biological systems with sub-cellular resolution. In this contribution, we have discussed several key factors that are important in assessing the quality of probes for both chemists and biologists, including selectivity, kinetics, and reversibility of sensing reactions, quantum yield, wavelength, and Stokes shifts of fluorophores, solubility, membrane permeability, protein interference, turnover, and organelle specificity of probe molecules. We specifically highlighted the advantages of reversibility in sensing reactions and its application in ratio-metric probe design.

In the future, we hope that probe developers will focus not only on exploring new chemistries for sensing reactions but also on fine-tuning probes for biological applications. We believe that with further development in this field, small-molecule fluorescent probes will become useful complements to protein-based probes in redox biology studies.

#### Acknowledgments

The research was supported in part by the National Institutes of Health (R01-GM115622, R01-CA207701, R21-CA213535 to J.W., R01-AG045183, R01-AT009050, R21-EB022302, and DP1-DK113644 to M.C.W.) and the Welch Foundation (Q-1912 to M.C.W.).

#### Author Disclosure Statement

X.J., J.C., and J.W. are co-inventors of a patent application related to the RealThiol probe.



## References

1. Abo M, Minakami R, Miyano K, Kamiya M, Nagano T, Urano Y, and Sumimoto H. Visualization of phagosomal hydrogen peroxide production by a novel fluorescent probe that is localized via SNAP-tag labeling. *Anal Chem* 86: 5983–5990, 2014.
2. Abo M, Urano Y, Hanaoka K, Terai T, Komatsu T, and Nagano T. Development of a highly sensitive fluorescence probe for hydrogen peroxide. *J Am Chem Soc* 133: 10629–10637, 2011.
3. Ahn Y-H, Lee J-S, and Chang Y-T. Combinatorial rosamine library and application to in vivo glutathione probe. *J Am Chem Soc* 129: 4510–4511, 2007.
4. Albers AE, Dickinson BC, Miller EW, and Chang CJ. A red-emitting naphthofluorescein-based fluorescent probe for selective detection of hydrogen peroxide in living cells. *Bioorg Med Chem Lett* 18: 5948–5950, 2008.
5. Albers AE, Okreglak V, and Chang CJ. A FRET-based approach to ratiometric fluorescence detection of hydrogen peroxide. *J Am Chem Soc* 128: 9640–9641, 2006.
6. Aller I, Rouhier N, and Meyer AJ. Development of roGFP2-derived redox probes for measurement of the glutathione redox potential in the cytosol of severely glutathione-deficient *rm11* seedlings. *Front Plant Sci* 4: 506, 2013.
7. Arai S, Lee S, Zhai D, Suzuki M, and Chang YT. A molecular fluorescent probe for targeted visualization of temperature at the endoplasmic reticulum. *Sci Reports* 4: 6701, 2014.
8. Ashton TD, Jolliffe KA, and Pfeffer FM. Luminescent probes for the bioimaging of small anionic species in vitro and in vivo. *Chem Soc Rev* 44: 4547–4595, 2015.
9. Belousov VV, Fradkov AF, Lukyanov KA, Staroverov DB, Shakhbazov K, Tersikh AV, and Lukyanov S. Genetically encoded fluorescent indicator for intracellular hydrogen peroxide. *Nat Methods* 3: 281–286, 2006.
10. Best MD. Click chemistry and bioorthogonal reactions: unprecedented selectivity in the labeling of biological molecules. *Biochemistry* 48: 6571–6584, 2009.
11. Best QA, Sattenapally N, Dyer DJ, Scott CN, and McCarroll ME. pH-dependent Si-fluorescein hypochlorous acid fluorescent probe: spirocycle ring-opening and excess hypochlorous acid-induced chlorination. *J Am Chem Soc* 135: 13365–13370, 2013.
12. Bilan DS, Pase L, Joosen L, Gorokhovatsky AY, Erma-kova YG, Gadella TW, Grabher C, Schultz C, Lukyanov S, and Belousov VV. HyPer-3: a genetically encoded H<sub>2</sub>O<sub>2</sub> probe with improved performance for ratiometric and fluorescence lifetime imaging. *ACS Chem Biol* 8: 535–542, 2013.
13. Bruemmer KJ, Merrikhihaghi S, Lollar CT, Morris SNS, Bauer JH, and Lippert AR. 19F magnetic resonance probes for live-cell detection of peroxynitrite using an oxidative decarbonylation reaction. *Chem Commun* 50: 12311–12314, 2014.
14. Chan J, Dodani SC, and Chang CJ. Reaction-based small-molecule fluorescent probes for chemoselective bioimaging. *Nat Chem* 4: 973–984, 2012.
15. Chang MCY, Pralle A, Isacoff EY, and Chang CJ. A selective, cell-permeable optical probe for hydrogen peroxide in living cells. *J Am Chem Soc* 126: 15392–15393, 2004.
16. Chen J, Jiang X, Carroll S, Huang J, and Wang J. Theoretical and experimental investigation of thermodynamics and kinetics of thiol-michael addition reactions: a case study of reversible fluorescent probes for glutathione imaging in single cells. *Org Lett* 17: 5978–5981, 2015.
17. Chen J, Jiang X, Zhang C, MacKenzie K, Stossi F, Palzkill T, Wang MC, and Wang J. A Reversible Reaction-Based Fluorescent Probe for Real-Time Imaging of Glutathione Dynamics in Mitochondria. *ACS Sens* 2: 1257–1261, 2017.
18. Chen J, Zhao M, Jiang X, Sizovs A, Wang MC, Provost CR, Huang J, and Wang J. Genetically anchored fluorescent probes for subcellular specific imaging of hydrogen sulfide. *Analyst* 141: 1209–1213, 2016.
19. Chen S, Chen ZJ, Ren W, and Ai HW. Reaction-based genetically encoded fluorescent hydrogen sulfide sensors. *J Am Chem Soc* 134: 9589–9592, 2012.
20. Chen W, Liu C, Peng B, Zhao Y, Pacheco A, and Xian M. New fluorescent probes for sulfane sulfurs and the application in bioimaging. *Chem Sci* 4: 2892–2896, 2013.
21. Chen X, Tian X, Shin I, and Yoon J. Fluorescent and luminescent probes for detection of reactive oxygen and nitrogen species. *Chem Soc Rev* 40: 4783–4804, 2011.
22. Chen X, Wang F, Hyun JY, Wei T, Qiang J, Ren X, Shin I, and Yoon J. Recent progress in the development of fluorescent, luminescent and colorimetric probes for detection of reactive oxygen and nitrogen species. *Chem Soc Rev* 45: 2976–3016, 2016.
23. Chen X, Zhong Z, Xu Z, Chen L, and Wang Y. 2',7'-Dichlorodihydrofluorescein as a fluorescent probe for reactive oxygen species measurement: forty years of application and controversy. *Free Radic Res* 44: 587–604, 2010.
24. Chen X, Zhou Y, Peng X, and Yoon J. Fluorescent and colorimetric probes for detection of thiols. *Chem Soc Rev* 39: 2120–2135, 2010.
25. Chen Y, Shi X, Lu Z, Wang X, and Wang Z. A Fluorescent probe for hydrogen peroxide in vivo based on the modulation of intramolecular charge transfer. *Anal Chem* 89: 5278–5284, 2017.
26. Chen ZJ, Ren W, Wright QE, and Ai HW. Genetically encoded fluorescent probe for the selective detection of peroxynitrite. *J Am Chem Soc* 135: 14940–14943, 2013.
27. Cheng D, Pan Y, Wang L, Zeng Z, Yuan L, Zhang X-B, and Chang YT. Selective visualization of the endogenous peroxynitrite in an inflamed mouse model by a mitochondria-targetable two-photon ratiometric fluorescent probe. *J Am Chem Soc* 139: 285–292, 2017.
28. Cheng W-Y, Tong H, Miller EW, Chang CJ, Remington J, Zucker RM, Bromberg PA, Samet JM, and Hofer TPJ. An integrated imaging approach to the study of oxidative stress generation by mitochondrial dysfunction in living cells. *Environ Health Perspect* 118: 902–908, 2010.
29. Cheng X, Jia H, Feng J, Qin J, and Li Z. “Reactive” probe for hydrogen sulfite: good ratiometric response and bioimaging application. *Sens Actuators B Chem* 184: 274–280, 2013.
30. Choi MG, Hwang J, Eor S, and Chang S-K. Chromogenic and fluorogenic signaling of sulfite by selective deprotection of resorufin levulinate. *Org Lett* 12: 5624–5627, 2010.
31. Chung C, Srikun D, Lim CS, Chang CJ, and Cho BR. A two-photon fluorescent probe for ratiometric imaging of hydrogen peroxide in live tissue. *Chem Commun* 47: 9618–9620, 2011.
32. Covarrubias L, Hernandezgarcia D, Schnabel D, Salas-Vidal E, and Castro-Obregon S. Function of reactive oxygen species during animal development: passive or active? *Dev Biol* 320: 1–11, 2008.

33. D' Autreaux B and Toledano MB. ROS as signalling molecules: mechanisms that generate specificity in ROS homeostasis. *Nat Rev Mol Cell Biol* 8: 813–824, 2007.
34. Dickinson BC and Chang CJ. A targetable fluorescent probe for imaging hydrogen peroxide in the mitochondria of living cells. *J Am Chem Soc* 130: 9638–9639, 2008.
35. Dickinson BC and Chang CJ. Chemistry and biology of reactive oxygen species in signaling or stress responses. *Nat Chem Biol* 7: 504–511, 2011.
36. Dickinson BC, Huynh C, and Chang CJ. A palette of fluorescent probes with varying emission colors for imaging hydrogen peroxide signaling in living cells. *J Am Chem Soc* 132: 5906–5915, 2010.
37. Dickinson BC, Tang Y, Chang Z, and Chang CJ. A nuclear-localized fluorescent hydrogen peroxide probe for monitoring sirtuin-mediated oxidative stress responses in vivo. *Chem Biol* 18: 943–948, 2011.
38. Dixon SJ and Stockwell BR. The role of iron and reactive oxygen species in cell death. *Nat Chem Biol* 10: 9–17, 2014.
39. Dooley CT, Dore TM, Hanson GT, Jackson WC, Remington SJ, and Tsien RY. Imaging dynamic redox changes in mammalian cells with green fluorescent protein indicators. *J Biol Chem* 279: 22284–22293, 2004.
40. Drummen GPC, Van Liebergen LCM, Op den Kamp JAF, and Post JA. C11-BODIPY(581/591), an oxidation-sensitive fluorescent lipid peroxidation probe: (micro)spectroscopic characterization and validation of methodology. *Free Radic Biol Med* 33: 473–490, 2002.
41. Du F, Min Y, Zeng F, Yu C, and Wu S. A Targeted and FRET-based ratiometric fluorescent nanoprobe for imaging mitochondrial hydrogen peroxide in living cells. *Small* 10: 964–972, 2014.
42. Durkop A and Wolfbeis OS. Nonenzymatic direct assay of hydrogen peroxide at neutral pH using the Eu3Tc fluorescent probe. *J Fluorescence* 15: 755–761, 2005.
43. Ellis HR and Poole LB. Novel application of 7-chloro-4-nitrobenzo-2-oxa-1,3-diazole to identify cysteine sulfenic acid in the AhpC component of alkyl hydroperoxide reductase. *Biochemistry* 36: 15013–15018, 1997.
44. Ermakova YG, Bilan DS, Matlashov ME, Mishina NM, Markvicheva KN, Subach OM, Subach FV, Bogeski I, Hoth M, and Enikolopov G. Red fluorescent genetically encoded indicator for intracellular hydrogen peroxide. *Nat Commun* 5: 5222, 2014.
45. Fairlamb AH and Cerami A. Metabolism and functions of trypanothione in the Kinetoplastida. *Annu Rev Microbiol* 46: 695–729, 1992.
46. Fan Y, and Ai H-W. Development of redox-sensitive red fluorescent proteins for imaging redox dynamics in cellular compartments. *Anal Bioanal Chem* 408: 2901–2911, 2016.
47. Fan Y, Makar M, Wang MX, and Ai HW. Monitoring thioredoxin redox with a genetically encoded red fluorescent biosensor. *Nat Chem Biol* 13: 1045–1052, 2017.
48. Filomeni G, De Zio D, and Cecconi F. Oxidative stress and autophagy: the clash between damage and metabolic needs. *Cell Death Differ* 22: 377–388, 2015.
49. Gandhi S and Abramov AY. Mechanism of oxidative stress in neurodegeneration. *Oxidative Med Cell Longevity* 2012:11, 2012.
50. Gautier A, Juillerat A, Heinis C, Correa IR, Kindermann M, Beaufils F, and Johnsson K. An engineered protein tag for multiprotein labeling in living cells. *Chem Biol* 15: 128–136, 2008.
51. George N, Pick H, Vogel H, Johnsson N, and Johnsson K. Specific labeling of cell surface proteins with chemically diverse compounds. *J Am Chem Soc* 126: 8896–8897, 2004.
52. Grimm JB, English BP, Chen J, Slaughter JP, Zhang Z, Revyakina A, Patel R, Macklin JJ, Normanno D, Singer RH, Lionnet T, and Lavis LD. A general method to improve fluorophores for live-cell and single-molecule microscopy. *Nat Methods* 12: 244–250, 2015.
53. Grimm JB, Heckman LM, and Lavis LD. The chemistry of small-molecule fluorogenic probes. *Prog Mol Biol Transl Sci* 113: 1–34, 2013.
54. Grimm JB, Muthusamy AK, Liang Y, Brown TA, Lemon WC, Patel R, Lu R, Macklin JJ, Keller PJ, Ji N, and Lavis LD. A general method to fine-tune fluorophores for live-cell and in vivo imaging. *Nat Methods* 14: 987–994, 2017.
55. Guo Z, Park S, Yoon J, and Shin I. Recent progress in the development of near-infrared fluorescent probes for bioimaging applications. *Chem Soc Rev* 43: 16–29, 2014.
56. Guohua J, Tengeng J, Xia L, Zheng W, Xiangxiang D, and Xiaohong W. Boronic acid functionalized N-doped carbon quantum dots as fluorescent probe for selective and sensitive glucose determination. *Mater Res Expr* 1: 025708, 2014.
57. Gupta V and Carroll KS. Sulfenic acid chemistry, detection and cellular lifetime. *Biochim Biophys Acta* 1840: 847–875, 2014.
58. Gupta V and Carroll KS. Rational design of reversible and irreversible cysteine sulfenic acid-targeted linear C-nucleophiles. *Chem Commun (Camb)* 52: 3414–3417, 2016.
59. Gupta V, Paritala H, and Carroll KS. Reactivity, selectivity, and stability in sulfenic acid detection: a comparative study of nucleophilic and electrophilic probes. *Bioconjug Chem* 27: 1411–1418, 2016.
60. Gutscher M, Pauleau A-L, Marty L, Brach T, Wabnitz GH, Samstag Y, Meyer AJ, and Dick TP. Real-time imaging of the intracellular glutathione redox potential. *Nat Methods* 5: 553–559, 2008.
61. Halliwell B. Biochemistry of oxidative stress. *Biochem Soc Trans* 35: 1147–1150, 2007.
62. Hitomi Y, Takeyasu T, Funabiki T, and Kodera M. Detection of enzymatically generated hydrogen peroxide by metal-based fluorescent probe. *Anal Chem* 83: 9213–9216, 2011.
63. Hong Y, Lam JWY, and Tang BZ. Aggregation-induced emission. *Chem Soc Rev* 40: 5361–5388, 2011.
64. Hu JJ, Wong N-K, Gu Q, Bai X, Ye S, and Yang D. HKOCI-2 series of green BODIPY-based fluorescent probes for hypochlorous acid detection and imaging in live cells. *Org Lett* 16: 3544–3547, 2014.
65. Ishikawa T, Li Z, Lu Y, and Rea PA. The GS-X pump in plant, yeast, and animal cells: structure, function, and gene expression. *Biosci Reports* 17: 189–207, 1997.
66. Jiang X, Chen J, Bajic A, Zhang C, Song X, Carroll SL, Cai Z-L, Tang M, Xue M, Cheng N, Schaaf CP, Li F, MacKenzie KR, Ferreone ACM, Xia F, Wang MC, Maletic-Savatic M, and Wang J. Quantitative real-time imaging of glutathione. *Nat Commun* 8: 16087, 2017.
67. Jiang X, Yu Y, Chen J, Zhao M, Chen H, Song X, Matzuk AJ, Carroll SL, Tan X, Sizovs A, Cheng N, Wang MC, and Wang J. Quantitative imaging of glutathione in live cells using a reversible reaction-based ratiometric fluorescent probe. *ACS Chem Biol* 10: 864–874, 2015.
68. Jiao X, Li Y, Niu J, Xie X, Wang X, and Tang B. Small-molecule fluorescent probes for imaging and detection of reactive oxygen, nitrogen, and sulfur species in biological systems. *Anal Chem* 90:533–555, 2018.

69. Jobsis PD, Rothstein EC, and Balaban RS. Limited utility of acetoxymethyl (AM)-based intracellular delivery systems, in vivo: interference by extracellular esterases. *J Microsc* 226: 74–81, 2007.
70. Kalyanaraman B, Darley-Usmar V, Davies KJA, Dennery PA, Forman HJ, Grisham MB, Mann GE, Moore K, Roberts II LJ, and Ischiropoulos H. Measuring reactive oxygen and nitrogen species with fluorescent probes: challenges and limitations. *Free Radic Biol Med* 52: 1–6, 2012.
71. Karlsson M, Kurz T, Brunk UT, Nilsson SE, and Frennesson CI. What does the commonly used DCF test for oxidative stress really show? *Biochem J* 428: 183–190, 2010.
72. Karton-Lifshin N, Segal E, Omer L, Portnoy M, Satchi-Fainaro R, and Shabat D. A unique paradigm for a Turn-ON near-infrared cyanine-based probe: noninvasive intravital optical imaging of hydrogen peroxide. *J Am Chem Soc* 133: 10960–10965, 2011.
73. Kaur A, Kolanowski JL, and New EJ. Reversible fluorescent probes for biological redox states. *Angew Chemie Int Ed* 55: 1602–1613, 2016.
74. Kaur M, Yang DS, Choi K, Cho MJ, and Choi DH. A fluorescence turn-on and colorimetric probe based on a diketopyrrolopyrrole–tellurophene conjugate for efficient detection of hydrogen peroxide and glutathione. *Dyes Pigments* 100: 118–126, 2014.
75. Keppler A, Gendrezig S, Gronemeyer T, Pick H, Vogel H, and Johnsson K. A general method for the covalent labeling of fusion proteins with small molecules in vivo. *Nat Biotechnol* 21: 86–89, 2003.
76. Kim D, Kim G, Nam S-J, Yin J, and Yoon J. Visualization of endogenous and exogenous hydrogen peroxide using a lysosome-targetable fluorescent probe. *Sci Reports* 5: 8488, 2015.
77. Kim G-J, Yoon D-H, Yun M-Y, Kwon H, Ha H-J, and Kim H-J. An activatable fluorescent probe for targeting cellular membrane through the biothiol-mediated hydrazone-to-pyrazole transformation. *Sens Actuators B Chem* 211: 245–249, 2015.
78. Koide Y, Kawaguchi M, Urano Y, Hanaoka K, Komatsu T, Abo M, Terai T, and Nagano T. A reversible near-infrared fluorescence probe for reactive oxygen species based on Tetrarhodamine. *Chem Commun* 48: 3091–3093, 2012.
79. Koide Y, Urano Y, Hanaoka K, Terai T, and Nagano T. Development of a Si-rhodamine-based far-red to near-infrared fluorescence probe selective for hypochlorous acid and its applications for biological imaging. *J Am Chem Soc* 133: 5680–5682, 2011.
80. Koide Y, Urano Y, Hanaoka K, Terai T, and Nagano T. Evolution of group 14 rhodamines as platforms for near-infrared fluorescence probes utilizing photoinduced electron transfer. *ACS Chem Biol* 6: 600–608, 2011.
81. Koide Y, Urano Y, Kenmoku S, Kojima H, and Nagano T. Design and synthesis of fluorescent probes for selective detection of highly reactive oxygen species in mitochondria of living cells. *J Am Chem Soc* 129: 10324–10325, 2007.
82. Kojima R, Takakura H, Kamiya M, Kobayashi E, Komatsu T, Ueno T, Terai T, Hanaoka K, Nagano T, and Urano Y. Development of a sensitive bioluminescent probe for imaging highly reactive oxygen species in living rats. *Angew Chem Int Ed* 54: 14981–14984, 2015.
83. Leonard SE, Reddie KG, and Carroll KS. Mining the thiol proteome for sulfenic acid modifications reveals new targets for oxidation in cells. *ACS Chem Biol* 4: 783–799, 2009.
84. Lepka K, Volbracht K, Bill E, Schneider R, Rios N, Hildebrandt T, Ingwersen J, Prozorovski T, Lillig CH, van Horssen J, Steinman L, Hartung HP, Radi R, Holmgren A, Aktas O, and Berndt C. Iron-sulfur glutaredoxin 2 protects oligodendrocytes against damage induced by nitric oxide release from activated microglia. *Glia* 65: 1521–1534, 2017.
85. Li C, Wu T, Hong C, Zhang G, and Liu S. A general strategy to construct fluorogenic probes from charge-generation polymers (CGPs) and AIE-active fluorogens through triggered complexation. *Angew Chem Int Ed* 51: 455–459, 2012.
86. Li G, Zhu D, Liu Q, Xue L, and Jiang H. Rapid detection of hydrogen peroxide based on aggregation induced ratiometric fluorescence change. *Org Lett* 15: 924–927, 2013.
87. Li X, Gao X, Shi W, and Ma H. Design strategies for water-soluble small molecular chromogenic and fluorogenic probes. *Chem Rev* 114: 590–659, 2014.
88. Li X, Tao R-R, Hong L-J, Cheng J, Jiang Q, Lu Y-M, Liao M-H, Ye W-F, Lu N-N, Han F, Hu Y-Z, and Hu Y-H. Visualizing peroxynitrite fluxes in endothelial cells reveals the dynamic progression of brain vascular injury. *J Am Chem Soc* 137: 12296–12303, 2015.
89. Li Z, Guo S, Yuan Z, and Lu C. Carbon quantum dot-gold nanocluster nanosatellite for ratiometric fluorescence probe and imaging for hydrogen peroxide in living cells. *Sens Actuators B Chem* 241: 821–827, 2016.
90. Liao Y-X, Li K, Wu M-Y, Wu T, and Yu X-Q. A selenium-contained aggregation-induced “turn-on” fluorescent probe for hydrogen peroxide. *Org Biomol Chem* 12: 3004–3008, 2014.
91. Lin K-K, Wu S-C, Hsu K-M, Hung C-H, Liaw W-F, and Wang Y-M. A N-(2-aminophenyl)-5-(dimethylamino)-1-naphthalenesulfonic amide (Ds-DAB) based fluorescent chemosensor for peroxynitrite. *Org Lett* 15: 4242–4245, 2013.
92. Lin VS, Dickinson BC, and Chang CJ. Boronate-based fluorescent probes: imaging hydrogen peroxide in living systems. *Methods Enzymol* 526: 19, 2013.
93. Lin W, Yuan L, Cao Z, Feng Y, and Long L. A sensitive and selective fluorescent thiol probe in water based on the conjugate 1,4-addition of thiols to  $\alpha$ ,  $\beta$ -unsaturated ketones. *Chemistry* 15: 5096–5103, 2009.
94. Liu B, Wang J, Zhang G, Bai R, and Pang Y. Flavone-based ESIPT ratiometric chemodosimeter for detection of cysteine in living cells. *ACS Appl Mater Interfaces* 6: 4402–4407, 2014.
95. Liu C, Chen W, Shi W, Peng B, Zhao Y, Ma H, and Xian M. Rational design and bioimaging applications of highly selective fluorescence probes for hydrogen polysulfides. *J Am Chem Soc* 136: 7257–7260, 2014.
96. Liu C, Pan J, Li S, Zhao Y, Wu LY, Berkman CE, Whorton AR, and Xian M. Capture and visualization of hydrogen sulfide by a fluorescent probe. *Angew Chem Int Ed* 50: 10327–10329, 2011.
97. Liu F, Wu T, Cao J, Zhang H, Hu M, Sun S, Song F, Fan J, Wang J, and Peng X. A novel fluorescent sensor for detection of highly reactive oxygen species, and for imaging such endogenous hROS in the mitochondria of living cells. *Analyst* 138: 775–778, 2013.
98. Liu G, Long Z, Lv H, Li C, and Xing G. A dialdehyde-diboronate-functionalized AIE luminogen: design, synthesis and application in the detection of hydrogen peroxide. *Chem Commun* 52: 10233–10236, 2016.

99. Liu H-W, Zhu X, Zhang J, Zhang X-B, and Tan W. A red emitting two-photon fluorescent probe for dynamic imaging of redox balance mediated by a superoxide anion and GSH in living cells and tissues. *Analyst* 141: 5893–5899, 2016.
100. Liu J, Ren J, Bao X, Gao W, Wu C, and Zhao Y. pH-switchable fluorescent probe for spatially-confined visualization of intracellular hydrogen peroxide. *Anal Chem* 88: 5865–5870, 2016.
101. Liu Z, Zhou X, Miao Y, Hu Y, Kwon N, Wu X, and Yoon J. A reversible fluorescent probe for real-time quantitative monitoring of cellular glutathione. *Angew Chem Int Ed* 56: 5812–5816, 2017.
102. Los GV, Encell LP, McDougall MG, Hartzell DD, Karassina N, Zimprich C, Wood MG, Learish R, Ohana RF, Urh M, Simpson D, Klaubert J, Bulleit RF, and Wood KV. HaloTag: a novel protein labeling technology for cell imaging and protein analysis. *ACS Chem Biol* 3: 373–382, 2008.
103. Lou Z, Li P, and Han K. Redox-responsive fluorescent probes with different design strategies. *Acc Chem Res* 48: 1358–1368, 2015.
104. Lou Z, Li P, Pan Q, and Han K. A reversible fluorescent probe for detecting hypochloric acid in living cells and animals: utilizing a novel strategy for effectively modulating the fluorescence of selenide and selenoxide. *Chem Commun* 49: 2445–2447, 2013.
105. Lukyanov KA and Belousov VV. Genetically encoded fluorescent redox sensors. *Biochim Biophys Acta* 1840: 745–756, 2014.
106. Maeda H, Fukuyasu Y, Yoshida S, Fukuda M, Saeki K, Matsuno H, Yamauchi Y, Yoshida K, Hirata K, and Miyamoto K. Fluorescent probes for hydrogen peroxide based on a non-oxidative mechanism. *Angew Chem Int Ed* 43: 2389–2391, 2004.
107. Masanta G, Heo CH, Lim CS, Bae SK, Cho BR, and Kim HM. A mitochondria-localized two-photon fluorescent probe for ratiometric imaging of hydrogen peroxide in live tissue. *Chem Commun* 48: 3518–3520, 2012.
108. Meyer AJ and Dick TP. Fluorescent protein-based redox probes. *Antioxid Redox Signal* 13: 621–650, 2010.
109. Miao J, Huo Y, Liu Q, Li Z, Shi H, Shi Y, and Guo W. A new class of fast-response and highly selective fluorescent probes for visualizing peroxynitrite in live cells, subcellular organelles, and kidney tissue of diabetic rats. *Biomaterials* 107: 33–43, 2016.
110. Miller EW, Albers AE, Pralle A, Isacoff EY, and Chang CJ. Boronate-based fluorescent probes for imaging cellular hydrogen peroxide. *J Am Chem Soc* 127: 16652–16659, 2005.
111. Miller EW and Chang CJ. Fluorescent probes for nitric oxide and hydrogen peroxide in cell signaling. *Curr Opin Chem Biol* 11: 620–625, 2007.
112. Mittler R, Vanderauwera S, Suzuki N, Miller G, Tognetti VB, Vandepoele K, Gollery M, Shulaev V, and Van Breusegem F. ROS signaling: the new wave? *Trends Plant Sci* 16: 300–309, 2011.
113. Montoya LA and Pluth MD. Organelle-targeted H<sub>2</sub>S probes enable visualization of the subcellular distribution of H<sub>2</sub>S donors. *Anal Chem* 88: 5769–5774, 2016.
114. Morgan B, Van Laer K, Owusu TNE, Ezerija D, Pastor-Flores D, Amponsah PS, Tursch A, and Dick TP. Real-time monitoring of basal H<sub>2</sub>O<sub>2</sub> levels with peroxiredoxin-based probes. *Nat Chem Biol* 12: 437–443, 2016.
115. Murphy MP. Selective targeting of bioactive compounds to mitochondria. *Trends Biotechnol* 15: 326–330, 1997.
116. Narayanaswamy N, Narra S, Nair RR, Saini DK, Kon-daihb P, and Govindaraju T. Stimuli-responsive colorimetric and NIR fluorescence combination probe for selective reporting of cellular hydrogen peroxide. *Chem Sci* 7: 2832–2841, 2016.
117. Neef AB and Schultz C. Selective fluorescence labeling of lipids in living cells. *Angew Chem Int Ed* 48: 1498–1500, 2009.
118. Newton GL, Buchmeier N, and Fahey RC. Biosynthesis and functions of mycothiol, the unique protective thiol of Actinobacteria. *Microbiol Mol Biol Rev* 72: 471–494, 2008.
119. Newton GL, Rawat M, La Clair JJ, Jothivasan VK, Budiarto T, Hamilton CJ, Claiborne A, Helmann JD, and Fahey RC. Bacillithiol is an antioxidant thiol produced in Bacilli. *Nat Chem Biol* 5: 625–627, 2009.
120. Oshiki D, Kojima H, Terai T, Arita M, Hanaoka K, Urano Y, and Nagano T. Development and application of a near-infrared fluorescence probe for oxidative stress based on differential reactivity of linked cyanine dyes. *J Am Chem Soc* 132: 2795–2801, 2010.
121. Pan J and Carroll KS. Chemical biology approaches to study protein cysteine sulfenylation. *Biopolymers* 101: 165–172, 2014.
122. Peng T, Wong N-K, Chen X, Chan Y-K, Ho DH-H, Sun Z-N, Hu JJ, Shen J-G, El-Nezami H, and Yang D. Molecular imaging of peroxynitrite with HKGreen-4 in live cells and tissues. *J Am Chem Soc* 136: 11728–11734, 2014.
123. Prunty MC, Aung MH, Hanif AM, Allen RS, Chrenek MA, Boatright JH, Thule PM, Kundu K, Murthy N and Pardue MT. In vivo imaging of retinal oxidative stress using a reactive oxygen species-activated fluorescent probe. *Invest Ophthalmol Vis Sci* 56: 5862–5870, 2015.
124. Reja SI, Gupta M, Gupta N, Bhalla V, Ohri P, Kaur G, and Kumar M. A lysosome targetable fluorescent probe for endogenous imaging of hydrogen peroxide in living cells. *Chem Commun* 53: 3701–3704, 2017.
125. Ren W and Ai H. Genetically encoded fluorescent redox probes. *Sensors* 13: 15422–15433, 2013.
126. Resch-Genger U, Grabolle M, Cavaliere-Jaricot S, Nitschke R, and Nann T. Quantum dots versus organic dyes as fluorescent labels. *Nat Methods* 5: 763–775, 2008.
127. Rhee SG, Chang T-S, Jeong W, and Kang D. Methods for detection and measurement of hydrogen peroxide inside and outside of cells. *Mol Cells* 29: 539–549, 2010.
128. Rios N, Piacenza L, Trujillo M, Martinez A, Demicheli V, Prolo C, Alvarez MN, Lopez GV, and Radi R. Sensitive detection and estimation of cell-derived peroxynitrite fluxes using fluorescein-boronate. *Free Radic Biol Med* 101: 284–295, 2016.
129. Saa L and Pavlov V. Enzymatic growth of quantum dots: applications to probe glucose oxidase and horseradish peroxidase and sense glucose. *Small* 8: 3449–3455, 2012.
130. Schieber M and Chandel Navdeep S. ROS function in redox signaling and oxidative stress. *Curr Biol* 24: R453–R462, 2014.
131. Schiedel M-S, Briehn CA, and Bauerle P. Single-compound libraries of organic materials: parallel synthesis and screening of fluorescent dyes. *Angew Chem Int Ed* 40: 4677–4680, 2001.
132. Seo YH and Carroll KS. Facile synthesis and biological evaluation of a cell-permeable probe to detect redox-regulated proteins. *Bioorg Med Chem Lett* 19: 356–359, 2009.
133. Shan X, Chai L, Ma J, Qian Z, Chen J, and Feng H. B-doped carbon quantum dots as a sensitive fluorescence probe for hydrogen peroxide and glucose detection. *Analyst* 139: 2322–2325, 2014.

134. Sharma P, Jha AB, Dubey RS, and Pessarakli M. Reactive oxygen species, oxidative damage, and antioxidative defense mechanism in plants under stressful conditions. *J Bot* 2012: 1–26, 2012.
135. Shibata A, Furukawa K, Abe H, Tsuneda S, and Ito Y. Rhodamine-based fluorogenic probe for imaging biological thiol. *Bioorg Med Chem Lett* 18: 2246–2249, 2008.
136. Sies H. Hydrogen peroxide as a central redox signaling molecule in physiological oxidative stress: oxidative eustress. *Redox Biol* 11: 613–619, 2017.
137. Sikora A, Zielonka J, Lopez M, Joseph J, and Kalyanaraman B. Direct oxidation of boronates by peroxynitrite: mechanism and implications in fluorescence imaging of peroxynitrite. *Free Radic Biol Med* 47: 1401–1407, 2009.
138. Soh N, Sakawaki O, Makihara K, Odo Y, Fukaminato T, Kawai T, Irie M, and Imato T. Design and development of a fluorescent probe for monitoring hydrogen peroxide using photoinduced electron transfer. *Bioorg Med Chem* 13: 1131–1139, 2005.
139. Song D, Lim JM, Cho S, Park S-J, Cho J, Kang D, Rhee SG, You Y, and Nam W. A fluorescence turn-on H<sub>2</sub>O<sub>2</sub> probe exhibits lysosome-localized fluorescence signals. *Chem Commun* 48: 5449–5451, 2012.
140. Srikun D, Albers AE, and Chang CJ. A dendrimer-based platform for simultaneous dual fluorescence imaging of hydrogen peroxide and pH gradients produced in living cells. *Chem Sci* 2: 1156–1165, 2011.
141. Sun X, Xu Q, Kim G, Flower SE, Lowe JP, Yoon J, Fossey JS, Qian X, Bull SD, and James TD. A water-soluble boronate-based fluorescent probe for the selective detection of peroxynitrite and imaging in living cells. *Chem Sci* 5: 3368–3373, 2014.
142. Sun Z-N, Wang H-L, Liu F-Q, Chen Y, Tam PKH, and Yang D. BODIPY-based fluorescent probe for peroxynitrite detection and imaging in living cells. *Org Lett* 11: 1887–1890, 2009.
143. Tanaka F, Mase N, and Barbas CF. Determination of cysteine concentration by fluorescence increase: reaction of cysteine with a fluorogenic aldehyde. *Chem Commun* 15: 1762–1763, 2004.
144. Tang Y, Lee D, Wang J, Li G, Yu J, Lin W, and Yoon J. Development of fluorescent probes based on protection–deprotection of the key functional groups for biological imaging. *Chem Soc Rev* 44: 5003–5015, 2015.
145. Terai T and Nagano T. Small-molecule fluorophores and fluorescent probes for bioimaging. *Pflügers Arch* 465: 347–359, 2013.
146. Tian H, Qian J, Sun Q, Jiang C, Zhang R, and Zhang W. A coumarin-based fluorescent probe for differential identification of sulfide and sulfite in CTAB micelle solution. *Analyst* 139: 3373–3377, 2014.
147. Tian L, Yang Y, Wysocki LM, Arnold AC, Hu A, Ravichandran B, Sternson SM, Looger LL, and Lavis LD. Selective esterase–ester pair for targeting small molecules with cellular specificity. *Proc Natl Acad Sci U S A* 109: 4756–4761, 2012.
148. Tomin VI and Jaworski R. ESIPT from S<sub>2</sub> singlet state in 3-hydroxyflavone. *J Mol Struct* 924–926: 461–465, 2009.
149. Tsien RY. A non-disruptive technique for loading calcium buffers and indicators into cells. *Nature* 290: 527–528, 1981.
150. Tsien RY. Fluorescent probes of cell signaling. *Annu Rev Neurosci* 12: 227–253, 1989.
151. Umezawa K, Yoshida M, Kamiya M, Yamasoba T, and Urano Y. Rational design of reversible fluorescent probes for live-cell imaging and quantification of fast glutathione dynamics. *Nat Chem* 9: 279–286, 2017.
152. Vendrell M, Lee J, and Chang Y-T. Diversity-oriented fluorescence library approaches for probe discovery and development. *Curr Opin Chem Biol* 14: 383–389, 2010.
153. Vendrell M, Zhai D, Er JC, and Chang Y-T. Combinatorial strategies in fluorescent probe development. *Chem Rev* 112: 4391–4420, 2012.
154. Venkatesan P and Wu S-P. A turn-on fluorescent probe for hypochlorous acid based on the oxidation of diphenyl telluride. *Analyst* 140: 1349–1355, 2015.
155. Virgilio FD, Fasolato C, and Steinberg TH. Inhibitors of membrane transport system for organic anions block fura-2 excretion from PC12 and N2A cells. *Biochem J* 256: 959–963, 1988.
156. Virgilio FD, Steinberg TH, and Silverstein SC. Inhibition of Fura-2 sequestration and secretion with organic anion transport blockers. *Cell Calcium* 11: 57–62, 1990.
157. Wäldchen S, Lehmann J, Klein T, van de Linde S, and Sauer M. Light-induced cell damage in live-cell super-resolution microscopy. *Sci Reports* 5: 15348, 2015.
158. Wang B, Li P, Yu F, Song P, Sun X, Yang S, Lou Z, and Han K. A reversible fluorescence probe based on Se-BODIPY for the redox cycle between HClO oxidative stress and H<sub>2</sub>S repair in living cells. *Chem Commun* 49: 1014–1016, 2013.
159. Wang K, Peng H, and Wang B. Recent advances in thiol and sulfide reactive probes. *J Cell Biochem* 115: 1007–1022, 2014.
160. Wang X, Hu J, Zhang G, and Liu S. Highly selective fluorogenic multianalyte biosensors constructed via enzyme-catalyzed coupling and aggregation-induced emission. *J Am Chem Soc* 136: 9890–9893, 2014.
161. Wen Y, Liu K, Yang H, Li Y, Lan H, Liu Y, Zhang X, and Yi T. A highly sensitive ratiometric fluorescent probe for the detection of cytoplasmic and nuclear hydrogen peroxide. *Anal Chem* 86: 9970–9976, 2014.
162. Wen Y, Liu K, Yang H, Liu Y, Chen L, Liu Z, Huang C, and Yi T. Mitochondria-directed fluorescent probe for the detection of hydrogen peroxide near mitochondrial DNA. *Anal Chem* 87: 10579–10584, 2015.
163. Wen Y, Xue F, Lan H, Li Z, Xiao S, and Yi T. Multicolor imaging of hydrogen peroxide level in living and apoptotic cells by a single fluorescent probe. *Biosens Bioelectron* 91: 115–121, 2017.
164. Winterbourn CC. The challenges of using fluorescent probes to detect and quantify specific reactive oxygen species in living cells. *Biochim Biophys Acta* 1840: 730–738, 2014.
165. Wu M-Y, Li K, Li C-Y, Hou J-T, and Yu X-Q. A water-soluble near-infrared probe for colorimetric and ratiometric sensing of SO<sub>2</sub> derivatives in living cells. *Chem Commun* 50: 183–185, 2014.
166. Wysocki LM and Lavis LD. Advances in the chemistry of small molecule fluorescent probes. *Curr Opin Chem Biol* 15: 752–759, 2011.
167. Xiao H, Liu X, Wu C, Wu Y, Li P, Guo X, and Tang B. A new endoplasmic reticulum-targeted two-photon fluorescent probe for imaging of superoxide anion in diabetic mice. *Biosens Bioelectron* 91: 449–455, 2017.
168. Xie X, Li M, Tang F, Li Y, Zhang L, Jiao X, Wang X, and Tang B. Combinatorial strategy to identify fluorescent probes for biothiol and thiophenol based on diversified pyrimidine moieties and their biological applications. *Anal Chem* 89: 3015–3020, 2017.

169. Xie X, Yang Xe, Wu T, Li Y, Li M, Tan Q, Wang X, and Tang B. Rational design of an alpha-ketoamide-based near-infrared fluorescent probe specific for hydrogen peroxide in living systems. *Anal Chem* 88: 8019–8025, 2016.
170. Xu J, Zhai J, Xu Y, Zhu J, Qin Y, and Jiang D. A near-infrared fluorescent aza-bodipy probe for dual-wavelength detection of hydrogen peroxide in living cells. *Analyst* 141: 2380–2383, 2016.
171. Xu J, Zhang Y, Yu H, Gao X, and Shao S. Mitochondria-targeted fluorescent probe for imaging hydrogen peroxide in living cells. *Anal Chem* 88: 1455–1461, 2016.
172. Xu K, Tang B, Huang H, Yang G, Chen Z, Li P, and An L. Strong red fluorescent probes suitable for detecting hydrogen peroxide generated by mice peritoneal macrophages. *Chem Commun* 48: 5974–5976, 2005.
173. Yang D, Wang H-L, Sun Z-N, Chung N-W, and Shen J-G. A highly selective fluorescent probe for the detection and imaging of peroxynitrite in living cells. *J Am Chem Soc* 128: 6004–6005, 2006.
174. Yang Y, Bazhin AV, Werner J, and Karakhanova S. Reactive oxygen species in the immune system. *Int Rev Immunol* 32: 249–270, 2013.
175. Yi L, Li H, Sun L, Liu L, Zhang C, and Xi Z. A highly sensitive fluorescence probe for fast thiol-quantification assay of glutathione reductase. *Angew Chem Int Ed* 48: 4034–4037, 2009.
176. Yin H, Li H, Xia G, Ruan C, Shi Y, Wang H, Jin M, and Ding D. A novel non-fluorescent excited state intramolecular proton transfer phenomenon induced by intramolecular hydrogen bonds: an experimental and theoretical investigation. *Sci Reports* 6: 19774, 2016.
177. Yin J, Straight PD, McLoughlin SM, Zhou ZF, Lin AJ, Golan DE, Kelleher NL, Kolter R, and Walsh CT. Genetically encoded short peptide tag for versatile protein labeling by Sfp phosphopantetheinyl transferase. *Proc Natl Acad Sci U S A* 102: 15815–15820, 2005.
178. Yu C, Luo M, Zeng F, and Wu S. A fast-responding fluorescent turn-on sensor for sensitive and selective detection of sulfite anions. *Anal Methods* 4: 2638–2640, 2012.
179. Yu F, Li P, Li G, Zhao G, Chu T, and Han K. A Near-IR reversible fluorescent probe modulated by selenium for monitoring peroxynitrite and imaging in living cells. *J Am Chem Soc* 133: 11030–11033, 2011.
180. Yu F, Li P, Song P, Wang B, Zhao J, and Han K. Facilitative functionalization of cyanine dye by an on-off-on fluorescent switch for imaging of H<sub>2</sub>O<sub>2</sub> oxidative stress and thiols reducing repair in cells and tissues. *Chem Commun* 48: 4980–4982, 2012.
181. Yu F, Li P, Wang B, and Han K. Reversible near-infrared fluorescent probe introducing tellurium to mimetic glutathione peroxidase for monitoring the redox cycles between peroxynitrite and glutathione in vivo. *J Am Chem Soc* 135: 7674–7680, 2013.
182. Yu F, Song P, Li P, Wang B, and Han K. A fluorescent probe directly detect peroxynitrite based on boronate oxidation and its applications for fluorescence imaging in living cells. *Analyst* 137: 3740–3749, 2012.
183. Yuan L, Lin W, Zheng K, and Zhu S. FRET-based small-molecule fluorescent probes: rational design and bioimaging applications. *Acc Chem Res* 46: 1462–1473, 2013.
184. Yuan L, Wang L, Agrawalla BK, Park S-L, Zhu H, Sivaraman B, Peng J, Xu Q-H, and Chang YT. Development of targetable two-photon fluorescent probes to image hypochlorous Acid in mitochondria and lysosome in live cell and inflamed mouse model. *J Am Chem Soc* 137: 5930–5938, 2015.
185. Zeng YL, Wang YJ, Su ZH, and Tang CR. Determination of hydrogen peroxide residue in food using CdS quantum dots as fluorescence probes. *Adv Mater Res* 455–456: 1189–1194, 2012.
186. Zhang D, Macinkovic I, Devarie-Baez NO, Pan J, Park C-M, Carroll KS, Filipovic MR, and Xian M. Detection of protein S-sulfhydration by a tag-switch technique. *Angew Chem Int Ed* 53: 575–581, 2014.
187. Zhang H, Liu J, Liu C, Yu P, Sun M, Yan X, Guo J-P, and Guo W. Imaging lysosomal highly reactive oxygen species and lighting up cancer cells and tumors enabled by a Si-rhodamine-based near-infrared fluorescent probe. *Biomaterials* 133: 60–69, 2017.
188. Zhang Q, Zhu Z, Zheng Y, Cheng J, Zhang N, Long Y-T, Zheng J, Qian X, and Yang Y. A three-channel fluorescent probe that distinguishes peroxynitrite from hypochlorite. *J Am Chem Soc* 134: 18479–18482, 2012.
189. Zhang W, Liu W, Li P, Huang F, Wang H, and Tang B. Rapid-response fluorescent probe for hydrogen peroxide in living cells based on increased polarity of C-B bonds. *Anal Chem* 87: 9825–9828, 2015.
190. Zhao J, Ji S, Chen Y, Guo H, and Yang P. Excited state intramolecular proton transfer (ESIPT): from principal photophysics to the development of new chromophores and applications in fluorescent molecular probes and luminescent materials. *Phys Chem Chem Phys* 14: 8803–8817, 2012.
191. Zhou L, Peng Y, Wang Q, and Lin Q. An ESIPT-based two-photon fluorescent probe detection of hydrogen peroxide in live cells and tissues. *J Photochem Photobiol B Biol* 167: 264–268, 2017.
192. Zhou X, Kwon Y, Kim G, Ryu J-H, and Yoon J. A ratiometric fluorescent probe based on a coumarin-hemicyanine scaffold for sensitive and selective detection of endogenous peroxynitrite. *Biosens Bioelectron* 64: 285–291, 2015.
193. Zhu H, Fan J, Wang J, Mu H, and Peng X. An “enhanced PET”-based fluorescent probe with ultrasensitivity for imaging basal and elesclomol-induced HClO in cancer cells. *J Am Chem Soc* 136: 12820–12823, 2014.

Address correspondence to:

Dr. Jin Wang

Department of Pharmacology and Chemical Biology

Baylor College of Medicine

Houston, TX 77030-3411

E-mail: wangj@bcm.edu

Date of first submission to ARS Central, December 26, 2017;  
date of acceptance, January 7, 2018.

#### Abbreviations Used

ABC = ATP-binding cassette  
 AIE = aggregation induced emission  
 AM = acetylmethoxyl  
 Cys = cysteine  
 DCF = dichlorofluorescein  
 DCFH = dichlorodihydrofluorescein  
 ESIPT = excited state intramolecular proton transfer

**Abbreviations Used (Cont.)**

FRET = Förster resonance energy transfer  
GPC = gel permeation chromatography  
Grx = glutaredoxin  
GSH = glutathione  
GSSG = oxidized glutathione  
HClO = hypochlorous acid  
H<sub>2</sub>O<sub>2</sub> = hydrogen peroxide  
H<sub>2</sub>S = hydrogen sulfide  
Hyper = hydrogen peroxide sensor protein  
NIR = near-infrared

NO· = nitric oxide  
<sup>1</sup>O<sub>2</sub> = singlet oxygen  
O<sub>2</sub>·<sup>-</sup> = superoxide  
OCl<sup>-</sup> = hypochlorite  
OH· = hydroxyl radical  
ONOO<sup>-</sup> = peroxynitrite  
PF1 = peroxyfluor-1  
RNS = reactive nitrogen species  
roGFP = redox-sensitive green fluorescent protein  
ROS = reactive oxygen species  
TPP = triphenylphosphonium